



Fast multipole method for 3-D Poisson-Boltzmann equation in layered electrolyte-dielectric media



Bo Wang^{a,b}, Wenzhong Zhang^b, Wei Cai^{b,*}

^a LCSM(MOE), School of Mathematics and Statistics, Hunan Normal University, Changsha, Hunan, 410081, PR China

^b Department of Mathematics, Southern Methodist University, Dallas, TX 75275, USA

ARTICLE INFO

Article history:

Available online 26 April 2021

Keywords:

Fast multipole method
Poisson-Boltzmann equation
Layered media
Spherical harmonic expansion
Equivalent polarization source

ABSTRACT

In this paper, we propose a fast multipole method (FMM) for 3-D linearized Poisson-Boltzmann (PB) equation in layered electrolyte-dielectric media. We will extend our previous work on FMMs for Helmholtz and Laplace equations in layered media [1,2] to the case of electrolyte and dielectric layered media for applications arising from biophysics and colloidal fluids, such as ion channel transport and Helmholtz double layers. Two key mathematical formulas are developed for this purpose: Firstly, a Funk-Hecke formula for purely imaginary wave numbers is derived, which facilitates the derivation of multipole expansions of the potential far fields of charges in layered electrolyte-dielectric media. Secondly, a recurrence formula is constructed for run-time computations of the Sommerfeld-type integrals used in the FMM algorithm. Numerical results show that the proposed FMM for interactions of charges embedded in layered media under screened PB potentials has the same accuracy and the $O(N)$ computational complexity as the classic FMM for charge interactions in the free space.

© 2021 Elsevier Inc. All rights reserved.

1. Introduction

Layered electrolyte-dielectric media frequently occur in biological systems, e.g., ion channels [3], where ionic solvents and protein membrane create a layered environment around the ion channels. The interaction of charged particles in layered electrolyte-dielectric media, such as ions moving through ion channels or in Helmholtz double layers of electrolyte fluids, is governed by the Poisson-Boltzmann (PB) electrostatic potential. In a L -layer media with horizontal interfaces at $z = d_\ell$ and the l -th layer defined by

$$\Omega_\ell = \{\mathbf{r} = (x, y, z), x \in \mathbb{R}, y \in \mathbb{R}, d_\ell \leq z \leq d_{\ell-1}\} \quad (1.1)$$

where $d_L = -\infty$, $d_{-1} = \infty$, the potential of a charge at \mathbf{r}' is given by the Green's function of the PB or Poisson equation in the layered media which we denoted by $u_{\ell\ell'}(\mathbf{r}, \mathbf{r}')$ in this paper. It is the solution of the equation

$$\nabla^2 u_{\ell\ell'}(\mathbf{r}, \mathbf{r}') - \lambda_\ell^2 u_{\ell\ell'}(\mathbf{r}, \mathbf{r}') = -\frac{1}{\varepsilon_\ell} \delta(\mathbf{r}, \mathbf{r}'), \quad \mathbf{r} \in \Omega_\ell, \mathbf{r}' \in \Omega_{\ell'} \quad (1.2)$$

with the following jump conditions (denoted by $[\cdot]$):

* Corresponding author.

E-mail address: cai@smu.edu (W. Cai).

$$[u_{\ell\ell'}(\mathbf{r})] = 0, \quad \left[\varepsilon \frac{\partial u_{\ell\ell'}(\mathbf{r})}{\partial \mathbf{n}} \right] = 0, \quad \text{at } z = d_\ell, \quad (1.3)$$

for all $0 \leq \ell, \ell' \leq L$, where $\delta(\mathbf{r}, \mathbf{r}')$ is the Dirac delta function, ε_ℓ and λ_ℓ are the dielectric constant and the inverse Debye-Huckel length in the ℓ -th layer in the layered medium. In layers where $\lambda_\ell = 0$, such as in a membrane layer, we have the Poisson equation. For an 1:1 electrolyte solvent (monovalent:monovalent salts like NaCl),

$$\lambda \approx 0.33\sqrt{c_s} \text{ \AA}^{-1} \quad (1.4)$$

at room temperature (25 °C), c_s is the ionic concentration measured in molar units M, and $\text{\AA} = 10^{-10} \text{ m}$ (cf. [4]).

In a homogeneous ionic solvent, the Green's function of the linearized Poisson-Boltzmann equation is referred as the Yukawa potential or screened Coulomb potential (cf. [5,3,4]). The classic fast multipole method (FMM) for the Coulomb potential has been successfully extended to the Yukawa potential (cf. [6,7]) for the reduction of the $O(N^2)$ cost for computing the interactions between N particles (or sources) to $O(N)$, which has found many applications in computational biology, chemistry, colloidal sciences (cf. [8,9]). Similar to the FMM for the Coulomb potential [10,11], the mathematical foundation of the Yukawa-FMM is multipole expansions (MEs) based on addition theorems for modified Bessel functions. The MEs provide a low-rank approximation for far fields of charges in the homogeneous space (also referred as the free space in this paper). For applications involving layered electrolyte-dielectric media, a layered Green's function defined via (1.2)–(1.3) is preferred to describe the interactions, which accounts for the polarization effects due to the presence of material interfaces (cf. [3,12]). However, the lack of a similar addition theory for the Green's function of PB equation in layered media place a major obstacle in developing FMM for the potential in this situation.

However, besides the ME based FMMs, Taylor expansion based fast algorithms [13–15], kernel independent FMM (cf. [16, 17]), cylindrical wave decomposition together with 2-D FMMs for cylindrical waves [12], and matrix low rank representation based fast algorithms (cf. [18–22]) could also be applied to compute charge interaction potential in layered media. Though a smooth kernel satisfying some decaying conditions can be compressed using Taylor expansion, a truncated Taylor expansion with p -th order convergence for a 3-D problem will require $O(p^3)$ terms, compared with $O(p^2)$ for MEs. Other kernel independent fast algorithms require the computation of all entries (or those sampled using random row/column sampling approaches (cf. [21,22])) of the matrix, which is computationally prohibitive as each entry requires the computation of an oscillatory Sommerfeld-type integral. An $O(p^2)$ term ME based fast method, which takes advantage of the special geometry of the layered media and analytical properties of the Green's functions of the layered media in deriving the MEs will produce more efficient algorithms with rigorous error controls. Recently, we have developed a mathematical theory to obtain low-rank ME approximations for the far fields of source interactions represented by the layered Green's function of Helmholtz and Laplace equations (cf. [1,23,2]). The main idea is to use the generating function of the Bessel function (2-D case) or an extended Funk-Hecke formula (3-D case) to connect Bessel and plane wave functions, which facilitates the derivation of the required MEs. The reason of using plane wave expressions is that the layered Green's functions have Sommerfeld-type integral representations where the plane waves are involved. With the ME for far field approximations, corresponding FMMs for the layered Green's functions have been implemented. As the layered Green's function of the linearized Poisson-Boltzmann equation has a similar integral form as that of Helmholtz equation, we can extend our previous work on the FMMs of the Laplace and Helmholtz equations in layered media to PB equations.

A key result in this paper is an extension of the Funk-Hecke formula for purely imaginary wave numbers, which allows us to derive the MEs, local expansions (LEs) and multipole-to-local (M2L) translation operators for the reaction components of the PB layered Green's function. Under a similar framework proposed in our previous work, the potential due to sources embedded in layered media is decomposed into free space and reaction components, and equivalent polarization charges are introduced for each reaction component. The FMM in layered media will then consist of the existing Yukawa-FMM for the free space components, and newly introduced FMMs for the reaction components based on equivalent polarization sources and the corresponding layered MEs, LEs and M2L translation operators. Moreover, in order to avoid memory consuming pre-computed 3-D look-up tables (cf. [1]), we will develop a recurrence formula for efficient computation of the Sommerfeld-type integrals used in the algorithm. The resulting FMMs for the reaction field components are much faster than that for the free space components, as the introduced equivalent polarization charges are always separated from the associated target charges by a material interface. As a result, the proposed FMM for sources in layered electrolyte-dielectric media costs almost the same as the Yukawa-FMM for the problem in free space.

The rest of the paper is organized as follows. In Section 2, to provide the application background for the FMM for PB potentials in layered electrolyte-dielectric media, we introduce a charge interaction problem arising from computing the electrostatic potentials in a hybrid model for ion channel transport. Then, we present the formulas for the potential induced by sources embedded in layered electrolyte-dielectric media. As in our previous work on Helmholtz and Laplace equation, equivalent polarization charges for each type of the reaction components are introduced to represent the reaction components. In Section 3, we first make a short review of the key formulas on which the classic FMM-Yukawa algorithm relies. Then, the MEs, LEs and M2L translation operators for the reaction components are derived based on an extended Funk-Hecke formula which provides a spherical harmonic expansion for the exponential functions involved in the integral representation of the layered media Green's function of the PB equation. The FMMs for reaction components are constructed for the combined set of the original source charges and the equivalent polarization charges associated to each reaction component. In Section 4, we give numerical results to show the exponential accuracy and $O(N)$ complexity of the proposed

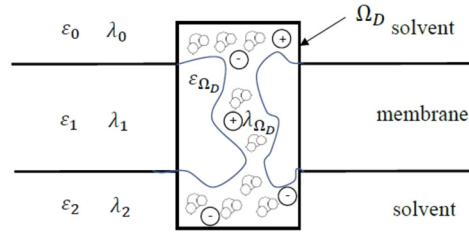


Fig. 2.1. Schematic illustration of a hybrid ion channel model: Ω_D indicates the atomistic region within which channel protein (indicated by curved outlines), water molecules (clusters of 2 hydrogen and 1 oxygen atoms), and ions (cations and anions indicated by + or -) are given in explicit atomistic forms in terms of charges and positions while the layered medium outside Ω_D given an implicit continuum form in terms of dielectric constant ε_ℓ and inverse Debye-Hückle length λ_ℓ .

FMM for interactions in layered electrolyte-dielectric media. A conclusion is given in Section 5. In addition, two appendices are included for the reaction densities in the spectrum domain for the Green's function for a three-layered medium and addition theorems for the modified Bessel functions, respectively.

2. Background and problem setup

2.1. Electrostatic interactions in a hybrid model for ion channel transport

As an application of the FMM in layered electrolyte-dielectric media, we present an computational electrostatic problem arising from the ion transport in ion-channel or nanopores. A three-layer medium of materials with different dielectric constants and inverse Debye-Hückle lengths, corresponding to ionic solvents above and below and a membrane in the middle, is shown in Fig. 2.1. In the layer Ω_ℓ , $0 \leq \ell \leq 2$, we denote the dielectric constants by ε_ℓ and the inverse Debye-Hückle lengths by λ_ℓ . For the study of ion channels, we consider a simple hybrid model within the layered medium, which consists of a cylinder Ω_D of height D within the three-layer medium with axis perpendicular to the interfaces of the layered media (see Fig. 2.1). The dielectric constant and inverse Debye-Hückle length inside the ion channel Ω_D are denoted by ε_{Ω_D} and $\lambda_{\Omega_D} = 0$ (i.e., Poisson equation is used inside the cylinder), respectively, which can take values different from the parameters outside the cylinder. The finite height cylinder represents a dividing interface in a hybrid solvation model for biomolecule simulations (refer to Section 4.5 in [4] and [24–27] for more details). In such a hybrid model, inside the cylinder an atomistic representation of the physical system is used, i.e., channel proteins, solvent molecules, and ions are described in terms of charged particles at their atomic centers and their interactions are governed by the Coulombic potential. The background media outside the cylinder, composed of a membrane and solvents above and below, are modeled as layered continuum dielectrics described by dielectric constants and Debye-Hückle screen length. The electrostatic potential in the layered media is then governed by the Poisson (for the membrane) and Poisson-Boltzmann (for the ionic solvents) equations.

Now, let us assume that inside the cylinder there are M charges with magnitudes q_k , $1 \leq k \leq M$, located at \mathbf{r}_k , which are the partial charges of the ions and membrane protein molecules inside the explicit atomistic cylinder. In a Monte Carlo or molecular dynamics simulation of the hybrid system, the electrostatic potential $\phi(\mathbf{r})$, thus forces on each charge through the gradient of the potential, is given by the following PB equation

$$\nabla^2 \phi(\mathbf{r}) - \lambda^2(\mathbf{r})\phi(\mathbf{r}) = -\frac{1}{\varepsilon(\mathbf{r})} \sum_{k=1}^M q_k \delta(\mathbf{r} - \mathbf{r}_k), \quad \mathbf{r} \in \Omega_\ell, \quad \ell = 0, 1, 2 \quad (2.1)$$

with interface conditions (1.3). The function $\lambda(\mathbf{r})$ is a perturbation of the piecewise constant λ_ℓ due to the presence of the cylinder representing the atomistic region, so

$$\lambda^2(\mathbf{r}) = \lambda_\ell^2 + \Delta(\mathbf{r})\chi_{\Omega_D}, \quad \Delta(\mathbf{r}) = \lambda_{\Omega_D}^2(\mathbf{r}) - \lambda_\ell^2, \quad \mathbf{r} \in \Omega_\ell, \quad (2.2)$$

and the dielectric constant $\varepsilon(\mathbf{r})$ will take different values in different regions (usually ε_{Ω_D} assuming a value between ε_{vac} and $4\varepsilon_{vac}$ with ε_{vac} being the vacuum dielectric constant), see Fig. 2.1. In the middle membrane layer and inside the cylinder, we have $\lambda_1 = 0, \lambda_{\Omega_D} = 0$, so the Poisson equation is in fact used both inside the membrane layer and the explicit cylinder region. The region outside the cylinder is treated implicitly with the homogeneous PB (within the ionic solvent above and below the membrane) or Poisson equation (within the membrane). The cylindrical boundary is a mathematical interface defining where the explicit regions end and the implicit region begins. The hybrid model allows the ion channel to be modeled with atomistic details and accuracy. For biological ion channels of thickness about 3 nm, the height of the cylinder is taken to be around 400 Å and the diameter in the order of 100 Å. Considering the fact that the biological ionic concentration c_s is in the range of milli – M (mM), which gives a Debye-Hückle length of 100 Å from (1.4), therefore, for this size of explicit region, the polarization effect of the solvent above and below the membrane will be strong on charges inside the cylinder, which is reflected in the definition of the Green's function in (1.2) through a solvent reaction field component as defined in (2.8).

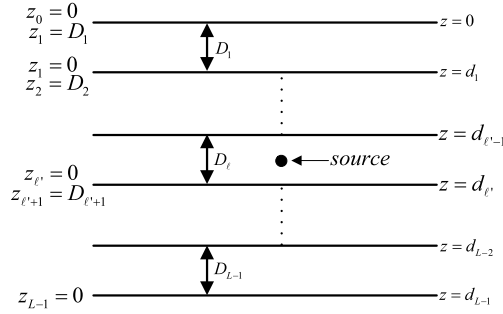


Fig. 2.2. Sketch of the layer structure for general multi-layer media.

The solution to (2.1) can be obtained by solving a Lipmann–Schwinger type integral equation using the Green’s function $u_{\ell\ell'}(\mathbf{r}, \mathbf{r}')$ defined by (1.2)-(1.3), i.e.,

$$\phi(\mathbf{r}) = -\frac{1}{\varepsilon(\mathbf{r})} \sum_{k=1}^M q_k u_{\ell\ell'}(\mathbf{r}, \mathbf{r}_k) + \int_{\Omega_D} \Delta(\mathbf{r}') u_{\ell\ell'}(\mathbf{r}, \mathbf{r}') \phi(\mathbf{r}') d\mathbf{r}', \quad \mathbf{r} \in \Omega_{\ell}. \tag{2.3}$$

The volume integral equation is then discretized by a Nyström collocation method with an appropriate quadrature formula with $\{\mathbf{r}_i, \omega_i\}_{i=1}^M$ as the nodes and weights for the domain Ω_D . More precisely, the discretization at each point $\mathbf{r}_i \in \Omega_D$, is given by

$$\phi(\mathbf{r}_i) = -\frac{1}{\varepsilon(\mathbf{r}_i)} \sum_{k=1}^M q_k u_{\ell\ell'}(\mathbf{r}_i, \mathbf{r}_k) + \sum_{j=1}^N \omega_j \Delta(\mathbf{r}_j) u_{\ell\ell'}(\mathbf{r}_i, \mathbf{r}_j) \phi(\mathbf{r}_j), \quad 1 \leq i \leq N, \tag{2.4}$$

which forms a linear system

$$(I + A\Lambda)\mathbf{x} = \mathbf{b}, \tag{2.5}$$

where $\mathbf{x} = (\phi(\mathbf{r}_1), \dots, \phi(\mathbf{r}_N))^T$, matrix $A = [u_{\ell\ell'}(\mathbf{r}_i, \mathbf{r}_j)]_{N \times N}$, $\ell = \ell' = 1$ is given by the layered Green’s function, $\Lambda = \text{diag}(\omega_1 \Delta(\mathbf{r}_1), \dots, \omega_M \Delta(\mathbf{r}_M))$ is a diagonal matrix and the right hand side $\mathbf{b} = (b_1, \dots, b_N)^T$, $b_i = \frac{1}{\varepsilon(\mathbf{r}_i)} \sum_{k=1}^M q_k u_{\ell\ell'}(\mathbf{r}_i, \mathbf{r}_k)$. Once the potential $\phi(\mathbf{r})$ is obtained inside Ω_D , then equation (2.3) can be used to find the potential anywhere in the layered medium. The linear system (2.5) is usually solved by using an iterative method when the system size N becomes very large. Iterative solvers based on Krylov subspace iterations such as GMRES require the product of the coefficient matrix and a vector, i.e., $A\Lambda\mathbf{x} \equiv A\mathbf{q}$, which will lead to $O(N^2)$ cost if done directly. Note that the product $A\mathbf{q}$ is exactly the interactions of N charges, defined by the $\mathbf{q} = (Q_1, \dots, Q_N)^T$, $Q_i = \omega_i \Delta(\mathbf{r}_i) x_i$, through the PB or Poisson electrostatic potential, i.e., the corresponding layered Green’s function. The speedup of computing the interaction from $O(N^2)$ to $O(N \log N)$ requires fast algorithm, such as the fast multipole method developed in this paper.

2.2. The potential due to sources embedded in layered media

In general, we will consider the computation of the potential due to sources in a multi-layered medium consisting of L -interfaces located at $z = d_{\ell}$, $\ell = 0, 1, \dots, L - 1$ with material parameters given by $\{\varepsilon_{\ell}, \lambda_{\ell}\}_{\ell=0}^L$, see Fig. 2.2. Suppose $\mathcal{P}_{\ell} = \{(Q_{\ell j}, \mathbf{r}_{\ell j}), j = 1, 2, \dots, N_{\ell}\}$, $\ell = 0, 1, \dots, L$ are $L + 1$ groups of source particles distributed in the multi-layered medium where the group of particles in the ℓ -th layer is denoted by \mathcal{P}_{ℓ} . Then, the potential at $\mathbf{r}_{\ell i}$ due to all other particles is given by

$$\Phi_{\ell}(\mathbf{r}_{\ell i}) = \sum_{\ell'=0}^L \sum_{j=1}^{N_{\ell'}} Q_{\ell' j} u_{\ell\ell'}(\mathbf{r}_{\ell i}, \mathbf{r}_{\ell' j}), \tag{2.6}$$

where $u_{\ell\ell'}(\mathbf{r}, \mathbf{r}')$ is the layered Green’s function, i.e., the solution of the problem (1.2)-(1.3).

As presented in our previous papers (cf. [1,2]), the potential consists of free space and reaction field components. To present the decomposed formulation of the potential, let us first recall the spectral representation of the Green’s function of PB equation in the layered medium described above. Suppose we have a point source at $\mathbf{r}' = (x', y', z')$ in the ℓ' -th layer ($d_{\ell'} < z' < d_{\ell'-1}$), then the layered Green’s function of the linearized PB equation satisfies (1.2) at field point $\mathbf{r} = (x, y, z)$ in the ℓ -th layer ($d_{\ell} < z < d_{\ell-1}$). By using partial Fourier transform along x - and y -directions, the analytical solution can be obtained by solving an ordinary differential equation in each layer with respect to z and then applying transmission

conditions (1.3) at the interfaces $z = d_{\ell-1}$, $\ell = 1, 2, \dots, L$, as well as decaying conditions in the top-most and bottom-most layers for $z \rightarrow \pm\infty$. The detailed derivation is an analogue to that for the layered Green's function of the Laplace equation (cf. [2]). In physical domain, the layered Green's function takes the form

$$u_{\ell\ell'}(\mathbf{r}, \mathbf{r}') = \begin{cases} u_{\ell\ell'}^{\text{react}}(\mathbf{r}, \mathbf{r}') + \frac{e^{-\lambda_\ell|\mathbf{r}-\mathbf{r}'|}}{4\pi\epsilon_\ell|\mathbf{r}-\mathbf{r}'|}, & \ell = \ell', \\ u_{\ell\ell'}^{\text{react}}(\mathbf{r}, \mathbf{r}'), & \text{otherwise,} \end{cases} \quad (2.7)$$

where

$$u_{\ell\ell'}^{\text{react}}(\mathbf{r}, \mathbf{r}') = \begin{cases} u_{0\ell'}^{11}(\mathbf{r}, \mathbf{r}') + u_{0\ell'}^{12}(\mathbf{r}, \mathbf{r}'), & \ell = 0 \\ u_{\ell\ell'}^{11}(\mathbf{r}, \mathbf{r}') + u_{\ell\ell'}^{12}(\mathbf{r}, \mathbf{r}') + u_{\ell\ell'}^{21}(\mathbf{r}, \mathbf{r}') + u_{\ell\ell'}^{22}(\mathbf{r}, \mathbf{r}'), & 0 < \ell < L, \\ u_{L\ell'}^{21}(\mathbf{r}, \mathbf{r}') + u_{L\ell'}^{22}(\mathbf{r}, \mathbf{r}'), & \ell = L \end{cases} \quad (2.8)$$

is a reaction field induced by the layered media. In general, the reaction components $u_{\ell\ell'}^{\text{ab}}(\mathbf{r}, \mathbf{r}')$, $a, b = 1, 2$, have Sommerfeld-type integral representations in the Fourier spectral domain:

$$u_{\ell\ell'}^{\text{ab}}(\mathbf{r}, \mathbf{r}') = \frac{1}{8\pi^2} \int_0^\infty \int_0^{2\pi} \frac{\lambda_\rho}{\lambda_{\ell z}} \mathcal{E}_{\ell\ell'}^{\text{ab}}(\mathbf{r}, \mathbf{r}') \sigma_{\ell\ell'}^{\text{ab}}(\lambda_\rho) d\alpha d\lambda_\rho, \quad a, b = 1, 2, \quad (2.9)$$

where $\lambda_{\ell z} = \sqrt{\lambda_\ell^2 + \lambda_\rho^2}$, $\{\mathcal{E}_{\ell\ell'}^{\text{ab}}(\mathbf{r}, \mathbf{r}')\}_{a,b=1,2}$ are exponential functions defined as

$$\begin{aligned} \mathcal{E}_{\ell\ell'}^{11}(\mathbf{r}, \mathbf{r}') &:= e^{i\lambda_\alpha \cdot (\boldsymbol{\rho} - \boldsymbol{\rho}') - \lambda_{\ell z}(z - d_\ell) - \lambda_{\ell' z}(z' - d_{\ell'})}, \\ \mathcal{E}_{\ell\ell'}^{12}(\mathbf{r}, \mathbf{r}') &:= e^{i\lambda_\alpha \cdot (\boldsymbol{\rho} - \boldsymbol{\rho}') - \lambda_{\ell z}(z - d_\ell) - \lambda_{\ell' z}(d_{\ell-1} - z')}, \\ \mathcal{E}_{\ell\ell'}^{21}(\mathbf{r}, \mathbf{r}') &:= e^{i\lambda_\alpha \cdot (\boldsymbol{\rho} - \boldsymbol{\rho}') - \lambda_{\ell z}(d_{\ell-1} - z) - \lambda_{\ell' z}(z' - d_{\ell'})}, \\ \mathcal{E}_{\ell\ell'}^{22}(\mathbf{r}, \mathbf{r}') &:= e^{i\lambda_\alpha \cdot (\boldsymbol{\rho} - \boldsymbol{\rho}') - \lambda_{\ell z}(d_{\ell-1} - z) - \lambda_{\ell' z}(d_{\ell-1} - z')}, \end{aligned} \quad (2.10)$$

$\lambda_\alpha = (\lambda_\rho \cos \alpha, \lambda_\rho \sin \alpha)$, $\boldsymbol{\rho} = (x, y)$, $\boldsymbol{\rho}' = (x', y')$ are the source and target coordinates in xy plane and $\{\sigma_{\ell\ell'}^{\text{ab}}(\lambda_\rho)\}_{a,b=1}^2$ are reaction densities only dependent on the layer structure and the material parameter κ_ℓ and ϵ_ℓ . It is noted that the reaction components $u_{\ell\ell'}^{\text{a}2}$ or $u_{\ell\ell'}^{\text{a}1}$ will vanish if the source is in the top-most or bottom-most layer accordingly.

The reaction densities $\{\sigma_{\ell\ell'}^{\text{ab}}(\lambda_\rho)\}_{a,b=1}^2$ can be calculated efficiently by using a recursive algorithm, see [2, Appendix B] for a similar one used for Laplace equation in layered media. For a few layers, we can write down explicit expressions of the reaction densities. As an example, the expressions for a general three layer medium are given in Appendix A.

With the expression of $u_{\ell\ell'}(\mathbf{r}, \mathbf{r}')$, the potential given by (2.6) is decomposed into free space and reaction field components as follows:

$$\Phi_\ell(\mathbf{r}_{\ell i}) = \Phi_\ell^{\text{free}}(\mathbf{r}_{\ell i}) + \sum_{\ell'=0}^{L-1} [\Phi_{\ell\ell'}^{11}(\mathbf{r}_{\ell i}) + \Phi_{\ell\ell'}^{21}(\mathbf{r}_{\ell i})] + \sum_{\ell'=1}^L [\Phi_{\ell\ell'}^{12}(\mathbf{r}_{\ell i}) + \Phi_{\ell\ell'}^{22}(\mathbf{r}_{\ell i})], \quad (2.11)$$

where

$$\Phi_\ell^{\text{free}}(\mathbf{r}_{\ell i}) := \sum_{j=1, j \neq i}^{N_\ell} Q_{\ell j} \frac{e^{-\lambda_\ell |\mathbf{r}_{\ell i} - \mathbf{r}_{\ell j}|}}{4\pi\epsilon_\ell |\mathbf{r}_{\ell i} - \mathbf{r}_{\ell j}|}, \quad \Phi_{\ell\ell'}^{\text{ab}}(\mathbf{r}_{\ell i}) := \sum_{j=1}^{N_{\ell'}} Q_{\ell' j} u_{\ell\ell'}^{\text{ab}}(\mathbf{r}_{\ell i}, \mathbf{r}_{\ell' j}). \quad (2.12)$$

It is clear that the free space component $\Phi_\ell^{\text{free}}(\mathbf{r}_{\ell i})$ can be computed using the classic Yukawa-FMM (cf. [6,7]). Therefore, the main task is to develop FMMs to efficiently compute the reaction components $\{\Phi_{\ell\ell'}^{\text{ab}}(\mathbf{r}_{\ell i})\}$, $a, b = 1, 2$. As the reaction components of the Green's function in layered media have different expressions (2.9) for source and target particles in different layers, it is necessary to perform calculation individually for interactions between any two groups of particles among the $L + 1$ groups $\{\mathcal{P}_\ell\}_{\ell=0}^L$.

2.3. Representation of the reaction components using equivalent polarization sources

According to the expressions in (2.9)–(2.10), we can see that the exponential decaying factors in (2.10) are actually determined by four groups of shifted z -coordinates $\{z - d_\ell, z' - d_{\ell'}\}$, $\{z - d_\ell, d_{\ell-1} - z'\}$, $\{d_{\ell-1} - z, z' - d_{\ell'}\}$ and $\{d_{\ell-1} - z, d_{\ell-1} - z'\}$. Based on this observation, our previous work on the Helmholtz equation [23,1] has shown that the exponential convergence of the ME and LE for the reaction components $u_{\ell\ell'}^{\text{ab}}(\mathbf{r}, \mathbf{r}')$ in fact depends on the distance between the target and a polarization source defined for the source at \mathbf{r}' . Fig. 2.3 illustrates the location of the polarization charge \mathbf{r}'_{ab} for each

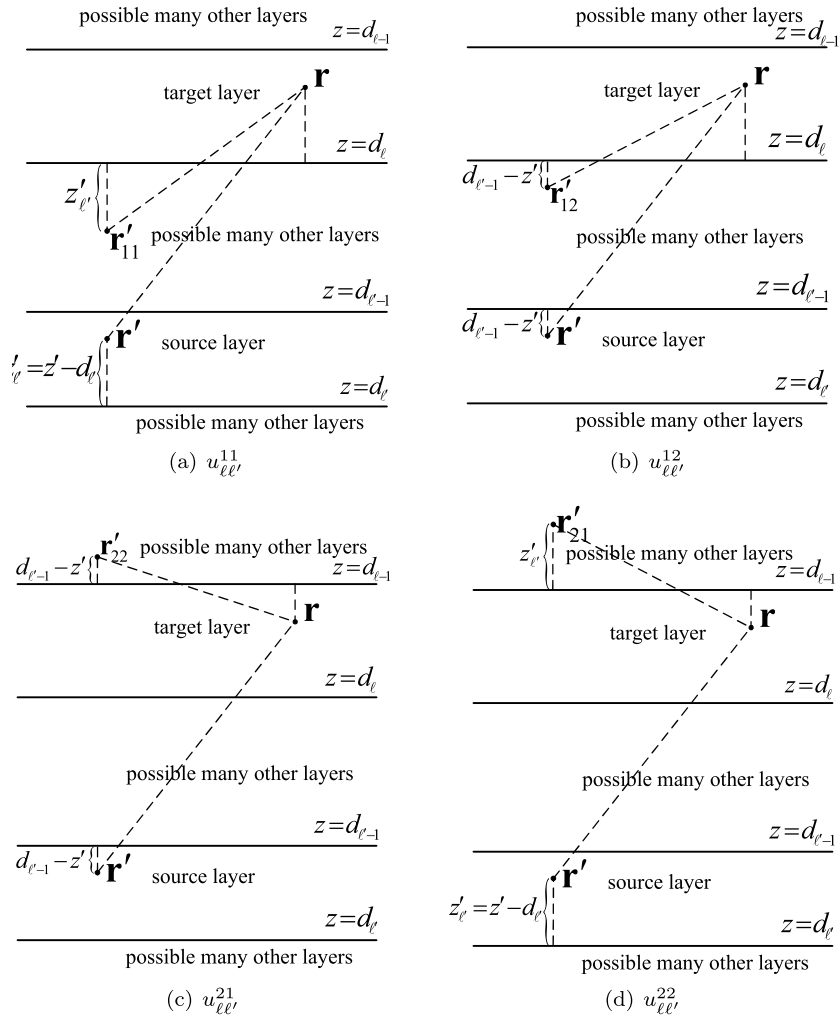


Fig. 2.3. Locations of equivalent polarization sources associated to reaction component $u_{\ell\ell'}^{ab}$.

of the four types of reaction fields $u_{\ell\ell'}^{ab}$, $a, b = 1, 2$. Specifically, the equivalent polarization sources associated to reaction components $u_{\ell\ell'}^{ab}(\mathbf{r}, \mathbf{r}')$, $a, b = 1, 2$ are set to be at coordinates (see Fig. 2.3)

$$\begin{aligned} \mathbf{r}'_{11} &:= (x', y', d_{\ell} - (z' - d_{\ell'})), & \mathbf{r}'_{12} &:= (x', y', d_{\ell} - (d_{\ell-1} - z')), \\ \mathbf{r}'_{21} &:= (x', y', d_{\ell-1} + (z' - d_{\ell'})), & \mathbf{r}'_{22} &:= (x', y', d_{\ell-1} + (d_{\ell-1} - z')), \end{aligned} \tag{2.13}$$

and the reaction potentials are defined as

$$\begin{aligned} \tilde{u}_{\ell\ell'}^{1b}(\mathbf{r}, \mathbf{r}'_{1b}) &:= \frac{1}{8\pi^2} \int_0^{\infty} \int_0^{2\pi} \frac{\lambda\rho}{\lambda_{\ell z}} \mathcal{E}_{\ell\ell'}^+(\mathbf{r}, \mathbf{r}'_{1b}) \sigma_{\ell\ell'}^{1b}(\lambda\rho) d\alpha d\lambda\rho, \\ \tilde{u}_{\ell\ell'}^{2b}(\mathbf{r}, \mathbf{r}'_{2b}) &:= \frac{1}{8\pi^2} \int_0^{\infty} \int_0^{2\pi} \frac{\lambda\rho}{\lambda_{\ell z}} \mathcal{E}_{\ell\ell'}^-(\mathbf{r}, \mathbf{r}'_{2b}) \sigma_{\ell\ell'}^{2b}(\lambda\rho) d\alpha d\lambda\rho, \end{aligned} \tag{2.14}$$

where

$$\begin{aligned} \mathcal{E}_{\ell\ell'}^+(\mathbf{r}, \mathbf{r}'_{1b}) &:= e^{i\lambda_{\alpha} \cdot (\rho - \rho'_{1b})} e^{-\lambda_{\ell z}(z - d_{\ell}) - \lambda_{\ell' z}(d_{\ell} - z'_{1b})}, \\ \mathcal{E}_{\ell\ell'}^-(\mathbf{r}, \mathbf{r}'_{2b}) &:= e^{i\lambda_{\alpha} \cdot (\rho - \rho'_{2b})} e^{-\lambda_{\ell z}(d_{\ell-1} - z) - \lambda_{\ell' z}(z'_{2b} - d_{\ell-1})}, \end{aligned} \tag{2.15}$$

and $\rho'_{ab} = (x'_{ab}, y'_{ab})$, z'_{ab} denote the xy - and z -coordinate of \mathbf{r}'_{ab} , respectively, i.e.,

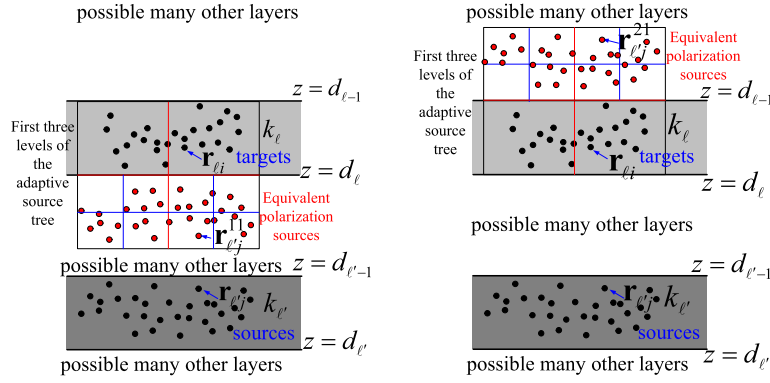


Fig. 2.4. Equivalent polarized sources $\{\mathbf{r}_{\ell'j}^{11}\}, \{\mathbf{r}_{\ell'j}^{21}\}$ and boxes in source tree.

$$\begin{aligned} z'_{11} &= d_\ell - (z' - d_{\ell'}), & z'_{12} &= d_\ell - (d_{\ell'-1} - z'), \\ z'_{21} &= d_{\ell-1} + (z' - d_{\ell'}), & z'_{22} &= d_{\ell-1} + (d_{\ell'-1} - z'). \end{aligned}$$

We can see that the reaction potentials (2.14) represented using the equivalent polarization sources has similar form as the Sommerfeld-type integral representation (2.9). Recalling the expressions (2.10), one can verify that

$$\mathcal{E}_{\ell\ell'}^{1b}(\mathbf{r}, \mathbf{r}') = \mathcal{E}^+(\mathbf{r}, \mathbf{r}'_{1b}), \quad \mathcal{E}_{\ell\ell'}^{2b}(\mathbf{r}, \mathbf{r}') = \mathcal{E}^-(\mathbf{r}, \mathbf{r}'_{2b}), \quad b = 1, 2. \quad (2.16)$$

Therefore, the reaction components of layered Green's function can be re-expressed using equivalent polarization coordinates as

$$u_{\ell\ell'}^{1b}(\mathbf{r}, \mathbf{r}') = \tilde{u}_{\ell\ell'}^{1b}(\mathbf{r}, \mathbf{r}'_{1b}), \quad u_{\ell\ell'}^{2b}(\mathbf{r}, \mathbf{r}') = \tilde{u}_{\ell\ell'}^{2b}(\mathbf{r}, \mathbf{r}'_{2b}), \quad b = 1, 2. \quad (2.17)$$

Substituting into the expression of $\Phi_{\ell\ell'}^{ab}(\mathbf{r}_{\ell i})$ in (2.12), we obtain

$$\Phi_{\ell\ell'}^{ab}(\mathbf{r}_{\ell i}) := \sum_{j=1}^{N_{\ell'}} Q_{\ell'j} \tilde{u}_{\ell\ell'}^{ab}(\mathbf{r}_{\ell i}, \mathbf{r}_{\ell'j}^{ab}), \quad a, b = 1, 2 \quad (2.18)$$

where

$$\begin{aligned} \mathbf{r}_{\ell'j}^{11} &= (x_{\ell'j}, y_{\ell'j}, d_\ell - (z_{\ell'j} - d_{\ell'})), & \mathbf{r}_{\ell'j}^{12} &= (x_{\ell'j}, y_{\ell'j}, d_\ell - (d_{\ell'-1} - z_{\ell'j})), \\ \mathbf{r}_{\ell'j}^{21} &= (x_{\ell'j}, y_{\ell'j}, d_{\ell-1} + (z_{\ell'j} - d_{\ell'})), & \mathbf{r}_{\ell'j}^{22} &= (x_{\ell'j}, y_{\ell'j}, d_{\ell-1} + (d_{\ell'-1} - z_{\ell'j})) \end{aligned} \quad (2.19)$$

are equivalent polarization coordinates of $\mathbf{r}_{\ell'j}$ for the computation of reaction components in the ℓ -th layer, see Fig. 2.4 for an illustration of $\{\mathbf{r}_{\ell'j}^{11}\}_{j=1}^{N_{\ell'}}$ and $\{\mathbf{r}_{\ell'j}^{21}\}_{j=1}^{N_{\ell'}}$.

By using the expression (2.18), the computation of the reaction components can be performed between targets and associated equivalent polarization sources. The definition given by (2.19) shows that the target particles $\{\mathbf{r}_{\ell i}\}_{i=1}^{N_\ell}$ and the corresponding equivalent polarization sources are always located on different sides of an interface $z = d_{\ell-1}$ or $z = d_\ell$, see Fig. 2.4. We want to emphasize that the introduced equivalent polarization sources are separated from the targets even in the computation of the reaction components for sources and targets in the same layer, see the numerical examples given in Section 3.2. This property implies significant advantage of introducing equivalent polarization sources and using expression (2.18) in the FMMs for the reaction components $\Phi_{\ell\ell'}^{ab}(\mathbf{r}_{\ell i})$, $a, b = 1, 2$. More details about this advantage will be discussed in Remark 3.3. The numerical results presented in Section 4 also validate that the FMMs for reaction components have high efficiency as a consequence of the separation of the targets and equivalent polarization sources by an interface.

3. FMM for charge interactions under PB potentials in 3-D layered media

In this section, we first briefly review the MEs and LEs for the free space Green's function of the linearized PB equation and the corresponding shifting/translation operators. They are the key formulas used in the Yukawa-FMM, which we will adopt for the computation of the free space components given in (2.12). Then, a new technique will be established to derive MEs, LEs and M2L translations for the general reaction components given by (2.18). With these expansions and translations, the FMM for the PB potentials (2.6) or their equivalent formulations (2.11) is proposed.

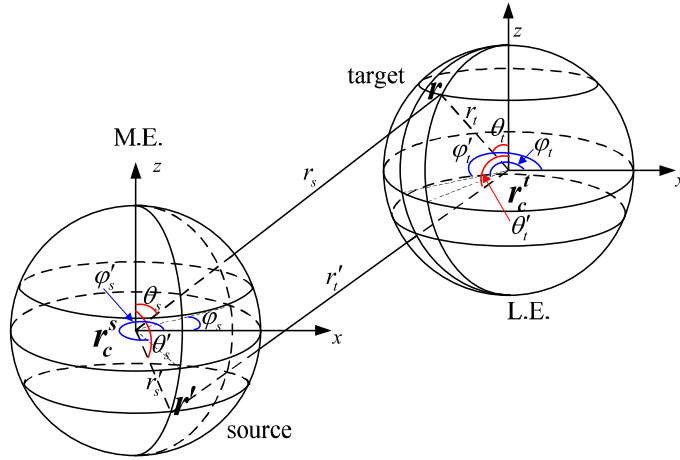


Fig. 3.1. Spherical coordinates used in multipole and local expansions.

3.1. Multipole and local expansions and translation operators for free-space components

Let us review the multipole and local expansions used in the Yukawa-FMM for Yukawa potential (cf. [6,7]). Consider the free space Green's function of the linearized PB equation with a source and a target at \mathbf{r}' and \mathbf{r} , respectively. By using the addition Theorem B.1, we obtain the ME with respect to a source center \mathbf{r}_c^s :

$$k_0(\lambda|\mathbf{r} - \mathbf{r}'|) = \frac{\pi}{2} \frac{e^{-\lambda|\mathbf{r} - \mathbf{r}'|}}{\lambda|\mathbf{r} - \mathbf{r}'|} = \sum_{n=0}^{\infty} \sum_{m=-n}^n M_{nm} k_n(\lambda r_s) Y_n^m(\theta_s, \varphi_s), \tag{3.1}$$

and the LE with respect to a target center \mathbf{r}_c^t :

$$k_0(\lambda|\mathbf{r} - \mathbf{r}'|) = \sum_{n=0}^{\infty} \sum_{m=-n}^n L_{nm} i_n(\lambda r_t) Y_n^m(\theta_t, \varphi_t), \tag{3.2}$$

where $\{Y_n^m(\theta, \varphi)\}$ are the spherical harmonic functions, $\{i_n(z)\}$ and $\{k_n(z)\}$ are the modified spherical Bessel functions of the first and second kind, respectively,

$$M_{nm} = 4\pi i_n(\lambda r_s') \overline{Y_n^m(\theta_s', \varphi_s')}, \quad L_{nm} = 4\pi k_n(\lambda r_t') Y_n^{-m}(\theta_t', \varphi_t'), \tag{3.3}$$

\mathbf{r}_c^s is the source center close to \mathbf{r}' , and \mathbf{r}_c^t is the target center close to \mathbf{r} , $(r_s, \theta_s, \varphi_s)$, $(r_t, \theta_t, \varphi_t)$ are the spherical coordinates of $\mathbf{r}' - \mathbf{r}_c^s$ and $\mathbf{r} - \mathbf{r}_c^t$, $(r_s', \theta_s', \varphi_s')$, $(r_t', \theta_t', \varphi_t')$ are the spherical coordinates of $\mathbf{r}' - \mathbf{r}_c^s$ and $\mathbf{r} - \mathbf{r}_c^t$ (see Fig. 3.1).

Applying the addition Theorem B.3 to $k_n(\lambda r_s) Y_n^m(\theta_s, \varphi_s)$ in (3.1), the translation from the ME (3.1) to the LE (3.2) is given by

$$L_{nm} = \sum_{\nu=0}^{\infty} \sum_{\mu=-\nu}^{\nu} S_{n\nu}^{m\mu}(\mathbf{r}_c^t - \mathbf{r}_c^s) M_{\nu\mu}. \tag{3.4}$$

Similarly, we can shift the centers of MEs and LEs via the following translations,

$$\tilde{M}_{nm} = \sum_{\nu=0}^{\infty} \sum_{\mu=-\nu}^{\nu} \overline{\widehat{S}_{n\nu}^{m\mu}(\mathbf{r}_c^s - \tilde{\mathbf{r}}_c^s)} M_{\nu\mu}, \quad \tilde{L}_{nm} = \sum_{\nu=0}^{\infty} \sum_{\mu=-\nu}^{\nu} \widehat{S}_{\nu n}^{\mu m}(\tilde{\mathbf{r}}_c^t - \mathbf{r}_c^t) L_{\nu\mu}, \tag{3.5}$$

where

$$\tilde{M}_{nm} = 4\pi i_n(\lambda \tilde{r}_s') \overline{Y_n^m(\tilde{\theta}_s', \tilde{\varphi}_s')}, \quad \tilde{L}_{nm} = 4\pi k_n(\lambda \tilde{r}_t') Y_n^m(\tilde{\theta}_t', \tilde{\varphi}_t') \tag{3.6}$$

are the coefficients of the ME and LE with respect to shifted centers $\tilde{\mathbf{r}}_s$ and $\tilde{\mathbf{r}}_t$, respectively.

Two important features in (3.1)–(3.2) are (i) the source and target coordinates are separated; (ii) they both have exponential convergence. These are the key features for the compression in the Yukawa-FMM (cf. [6,7]). Besides adopting the addition theorem, a new approach to handle Green's functions in layered media as well has been proposed for Helmholtz and Laplace equations (cf. [1,23,2]), which will be extended to PB equation below.

3.2. Multipole and local expansions and translation operators for a general reaction component

Before starting the derivation of the expansions for the general reaction components, we extend some expansion formulas which have been established for the development of the FMM for Helmholtz equation in layered media (cf. [1]).

We begin with an analytic extension of the well-known Funk–Hecke formula (cf. [28,29,1]).

Proposition 3.1. Given $\mathbf{r} = (x, y, z) \in \mathbb{R}^3$, $k > 0$, $\alpha \in [0, 2\pi)$ and denoted by (r, θ, φ) the spherical coordinates of \mathbf{r} , $\mathbf{k} = (\sqrt{k^2 - k_z^2} \cos \alpha, \sqrt{k^2 - k_z^2} \sin \alpha, k_z)$ is a vector of complex entries. Choosing branch (3.8) for $\sqrt{k^2 - k_z^2}$ in $e^{i\mathbf{k}\cdot\mathbf{r}}$ and $\widehat{P}_n^m(\frac{k_z}{k})$, we have

$$e^{i\mathbf{k}\cdot\mathbf{r}} = \sum_{n=0}^{\infty} \sum_{m=-n}^n A_n^m(\mathbf{r}) i^n \widehat{P}_n^m\left(\frac{k_z}{k}\right) e^{-im\alpha} = \sum_{n=0}^{\infty} \sum_{m=-n}^n \overline{A_n^m(\mathbf{r})} i^n \widehat{P}_n^m\left(\frac{k_z}{k}\right) e^{im\alpha} \tag{3.7}$$

holds for all $k_z \in \mathbb{C}$, where

$$A_n^m(\mathbf{r}) = 4\pi j_n(kr) Y_n^m(\theta, \varphi).$$

This extension enlarges the range of the classic Funk–Hecke formula from $k_z \in (-k, k)$ to the whole complex plane by choosing the branch

$$\sqrt{k^2 - k_z^2} = -i\sqrt{r_1 r_2} e^{i\frac{\theta_1 + \theta_2}{2}} \tag{3.8}$$

in the square root function $\sqrt{k^2 - k_z^2}$. Here (r_i, θ_i) , $i = 1, 2$ are the moduli and principal values of the arguments of complex numbers $k_z + k$ and $k_z - k$, i.e.,

$$k_z + k = r_1 e^{i\theta_1}, \quad -\pi < \theta_1 \leq \pi, \quad k_z - k = r_2 e^{i\theta_2}, \quad -\pi < \theta_2 \leq \pi.$$

There, it is enough to consider the case when $k > 0$ is a positive real number. Note that the linearized PB equation can be obtained from Helmholtz equation via modification $k \rightarrow i\lambda$. Therefore, it suffices to prove an alternative version of the Funk–Hecke formula for purely imaginary $k = i\lambda$.

By using the branch defined in (3.8) for the square root function, we have the extension (cf. [1]) of the well-known Legendre addition theorem [30, p. 395].

Lemma 3.1. Let $\mathbf{w} = (\sqrt{1 - w^2} \cos \alpha, \sqrt{1 - w^2} \sin \alpha, w)$ be a vector with complex components, θ, ϕ be the azimuthal angle and polar angles of a unit vector $\hat{\mathbf{r}}$. Define

$$\beta(w) = w \cos \theta + \sqrt{1 - w^2} \sin \theta \cos(\alpha - \phi), \tag{3.9}$$

then

$$P_n(\beta(w)) = \frac{4\pi}{2n + 1} \sum_{m=-n}^n \widehat{P}_n^m(\cos \theta) \widehat{P}_n^m(w) e^{im(\alpha - \phi)} \tag{3.10}$$

for all $w \in \mathbb{C}$.

The following Lemma states the same conclusion of Lemma 4 in [1]. Here, we make it more general by an analytic extension to \mathbb{C} .

Lemma 3.2. For any complex number a , there holds

$$e^{az} = \sum_{n=0}^{\infty} (2n + 1) i_n(a) P_n(z), \quad \forall z \in \mathbb{C}, \tag{3.11}$$

where $i_n(a) = \sqrt{\frac{\pi}{2a}} I_{n+1/2}(a)$ is the modified spherical Bessel function of the first kind, $P_n(z)$ is the Legendre polynomial extended to the complex plane.

Proof. Recall the series (cf. [31, 10.60.8])

$$e^{a \cos \theta} = \sum_{n=0}^{\infty} (2n + 1) i_n(a) P_n(\cos \theta), \tag{3.12}$$

we can see that (3.11) holds for all $z \in [-1, 1]$. Next, we consider its analytic extension to \mathbb{C} . Apparently, e^{az} is an entire function of z . Meanwhile, the spherical Bessel function $i_n(a)$ has the following upper bound (cf. [32, 9.1.62])

$$|i_n(a)| = |i^{-n} j_n(ia)| \leq \frac{\Gamma(\frac{3}{2})}{\Gamma(n + \frac{3}{2})} \left(\frac{a}{2}\right)^n e^{|\Re a|} \leq \frac{1}{n!} \left(\frac{a}{2}\right)^n e^{|\Re a|}, \tag{3.13}$$

where $\Re a$ is the real part of a . The extension of the Legendre polynomial $P_n(z)$ to \mathbb{C} is a polynomial of degree n with n distinct roots $\{z_j\}_{j=1}^n$ in the interval $[-1, 1]$. Therefore,

$$|P_n(z)| = |a_n| \prod_{j=1}^n |z - z_j| \leq 2^n (|z| + 1)^n, \quad \forall z \in \mathbb{C}, \tag{3.14}$$

here the estimate $a_n = \frac{(2n)!}{2^n (n!)^2} \leq 2^n$ for the coefficient of the leading term of $P_n(z)$ is used. In total, the upper bounds for $|i_n(a)|$ and $|P_n(z)|$ give an estimate

$$\sum_{n=0}^{\infty} (2n + 1) |i_n(a) P_n(z)| \leq \sum_{n=0}^{\infty} (2n + 1) \frac{a^n (|z| + 1)^n}{n!} e^{|\Re a|} = (2a(|z| + 1) + 1) e^{a(|z|+1)} e^{|\Re a|}. \tag{3.15}$$

Therefore, we have proved that the series on the right-hand side of (3.11) converges uniformly in any compact set $D \subset \mathbb{C}$ and hence converges to an entire function of z . By the analytic extension theory, we complete the proof. \square

From Lemma 3.1 and 3.2, we have the following expansion formulas:

Proposition 3.2. Given $\mathbf{r} = (x, y, z) \in \mathbb{R}^3$, $\lambda > 0$, $\alpha \in [0, 2\pi)$ and denote the spherical coordinates of \mathbf{r} by (r, θ, φ) , and let $\boldsymbol{\lambda} = (i\lambda_\rho \cos \alpha, i\lambda_\rho \sin \alpha, -\sqrt{\lambda^2 + \lambda_\rho^2})$ be a vector of complex entries. By choosing the branch (3.8) for $\lambda_z = \sqrt{\lambda^2 + \lambda_\rho^2}$ in $e^{i\boldsymbol{\lambda} \cdot \mathbf{r}}$ and $\widehat{P}_n^m(\frac{\lambda_z}{\lambda})$, we have

$$e^{\boldsymbol{\lambda} \cdot \mathbf{r}} = \sum_{n=0}^{\infty} \sum_{m=-n}^n \overline{B_n^m(\mathbf{r})} \widehat{P}_n^m\left(\frac{\lambda_z}{\lambda}\right) e^{im\alpha} = \sum_{n=0}^{\infty} \sum_{m=-n}^n B_n^m(\mathbf{r}) \widehat{P}_n^m\left(\frac{\lambda_z}{\lambda}\right) e^{-im\alpha} \tag{3.16}$$

for all $\lambda_\rho \in \mathbb{C}$, where

$$B_n^m(\mathbf{r}) = 4\pi (-1)^n i_n(\lambda r) Y_n^m(\theta, \varphi).$$

Proof. Let

$$\beta = \sqrt{1 + \frac{\lambda_\rho^2}{\lambda^2}} \cos \theta + i \frac{\lambda_\rho}{\lambda} \sin \theta \cos(\alpha - \phi),$$

then, $-\lambda r \beta = \boldsymbol{\lambda} \cdot \mathbf{r}$. Setting $a = \lambda r$, $z = \beta$ in (3.11), we have

$$e^{\boldsymbol{\lambda} \cdot \mathbf{r}} = \sum_{n=0}^{\infty} (2n + 1) i_n(-\lambda r) P_n(\beta). \tag{3.17}$$

Then, the spherical harmonic expansion (3.16) follows by applying Lemma 3.1 together with the property $i_n(-z) = (-1)^n i_n(z)$. \square

Now, we are ready to derive key mathematical formulas for the development of the FMM for a general reaction component $\Phi_{\ell\ell'}^{\text{ab}}(\mathbf{r}\ell i)$. We will use expression (2.18) with equivalent polarization coordinates. Therefore, MEs, LEs and corresponding translation operators for $\tilde{u}_{\ell\ell'}^{\text{ab}}(\mathbf{r}, \mathbf{r}'_{\text{ab}})$ are required. Recall that the source/target separation in the expansions is a key feature for the compression. Further, the coordinates of the equivalent polarization source and target are only involved in the exponential kernels $\mathcal{E}_{\ell\ell'}^{\pm}$ in the integral representation (2.14). Therefore, the following source/target separation

$$\begin{aligned} \mathcal{E}_{\ell\ell'}^+(\mathbf{r}, \mathbf{r}'_{1\text{b}}) &= \mathcal{E}_{\ell\ell'}^+(\mathbf{r}, \mathbf{r}_c^{1\text{b}}) e^{i\lambda_\alpha \cdot (\boldsymbol{\rho}_c^{1\text{b}} - \boldsymbol{\rho}'_{1\text{b}}) - \lambda_{\ell'z} (z_c^{1\text{b}} - z'_{1\text{b}})} \\ \mathcal{E}_{\ell\ell'}^-(\mathbf{r}, \mathbf{r}'_{2\text{b}}) &= \mathcal{E}_{\ell\ell'}^-(\mathbf{r}, \mathbf{r}_c^{2\text{b}}) e^{i\lambda_\alpha \cdot (\boldsymbol{\rho}_c^{2\text{b}} - \boldsymbol{\rho}'_{2\text{b}}) + \lambda_{\ell'z} (z_c^{2\text{b}} - z'_{2\text{b}})} \end{aligned} \tag{3.18}$$

and

$$\begin{aligned} \mathcal{E}_{\ell\ell'}^+(\mathbf{r}, \mathbf{r}'_{1\text{b}}) &= \mathcal{E}_{\ell\ell'}^+(\mathbf{r}_c^t, \mathbf{r}'_{1\text{b}}) e^{i\lambda_\alpha \cdot (\boldsymbol{\rho} - \boldsymbol{\rho}_c^t) - \lambda_{\ell z} (z - z_c)}, \\ \mathcal{E}_{\ell\ell'}^-(\mathbf{r}, \mathbf{r}'_{2\text{b}}) &= \mathcal{E}_{\ell\ell'}^-(\mathbf{r}_c^t, \mathbf{r}'_{2\text{b}}) e^{i\lambda_\alpha \cdot (\boldsymbol{\rho} - \boldsymbol{\rho}_c^t) + \lambda_{\ell z} (z - z_c)} \end{aligned} \tag{3.19}$$

can be obtained for $b = 1, 2$ by inserting the polarization source centers $\mathbf{r}_c^{ab} = (x_c^{ab}, y_c^{ab}, z_c^{ab})$ and the target center $\mathbf{r}_c^t = (x_c^t, y_c^t, z_c^t)$, respectively. Here we also use notations $\boldsymbol{\rho}_c^{ab} = (x_c^{ab}, y_c^{ab})$ and $\boldsymbol{\rho}_c^t = (x_c^t, y_c^t)$. Moreover, Proposition 3.2 gives spherical harmonic expansions:

$$\begin{aligned}
 e^{i\lambda\alpha \cdot (\boldsymbol{\rho}_c^{1b} - \boldsymbol{\rho}'_{1b}) - \lambda_{\ell'z}(z_c^{1b} - z'_{1b})} &= \sum_{n=0}^{\infty} \sum_{m=-n}^n 4\pi (-1)^n i_n(\lambda_{\ell'} r_s^{1b}) \overline{Y_n^m(\pi - \theta_s^{1b}, \pi + \varphi_s^{1b})} \widehat{P}_n^m\left(\frac{\lambda_{\ell'z}}{\lambda_{\ell'}}\right) e^{i\alpha}, \\
 e^{i\lambda\alpha \cdot (\boldsymbol{\rho}_c^{2b} - \boldsymbol{\rho}'_{2b}) + \lambda_{\ell'z}(z_c^{2b} - z'_{2b})} &= \sum_{n=0}^{\infty} \sum_{m=-n}^n 4\pi (-1)^n i_n(\lambda_{\ell'} r_s^{2b}) \overline{Y_n^m(\theta_s^{2b}, \pi + \varphi_s^{2b})} \widehat{P}_n^m\left(\frac{\lambda_{\ell'z}}{\lambda_{\ell'}}\right) e^{i\alpha}, \\
 e^{i\lambda\alpha \cdot (\boldsymbol{\rho}_c^t - \boldsymbol{\rho}'_c) - \lambda_{\ell z}(z - z'_c)} &= \sum_{n=0}^{\infty} \sum_{m=-n}^n 4\pi (-1)^n i_n(\lambda_{\ell} r_t) Y_n^m(\theta_t, \varphi_t) \widehat{P}_n^m\left(\frac{\lambda_{\ell z}}{\lambda_{\ell}}\right) e^{-i\alpha}, \\
 e^{i\lambda\alpha \cdot (\boldsymbol{\rho}_c^t - \boldsymbol{\rho}'_c) + \lambda_{\ell z}(z - z'_c)} &= \sum_{n=0}^{\infty} \sum_{m=-n}^n 4\pi (-1)^n i_n(\lambda_{\ell} r_t) Y_n^m(\pi - \theta_t, \varphi_t) \widehat{P}_n^m\left(\frac{\lambda_{\ell z}}{\lambda_{\ell}}\right) e^{-i\alpha},
 \end{aligned}$$

where $(r_s^{ab}, \theta_s^{ab}, \varphi_s^{ab})$ are the spherical coordinates of $\mathbf{r}'_{ab} - \mathbf{r}_c^{ab}$. Since

$$Y_n^m(\pi - \theta, \varphi) = (-1)^{n+m} Y_n^m(\theta, \varphi), \quad Y_n^m(\theta, \pi + \varphi) = (-1)^m Y_n^m(\theta, \varphi),$$

the above spherical harmonic expansions together with source/target separation (3.18) and (3.19) implies

$$\begin{aligned}
 \mathcal{E}_{\ell\ell'}^+(\mathbf{r}, \mathbf{r}'_{1b}) &= \mathcal{E}_{\ell\ell'}^+(\mathbf{r}, \mathbf{r}_c^{1b}) \sum_{n=0}^{\infty} \sum_{m=-n}^n 4\pi i_n(\lambda_{\ell'} r_s^{1b}) \overline{Y_n^m(\theta_s^{1b}, \varphi_s^{1b})} \widehat{P}_n^m\left(\frac{\lambda_{\ell'z}}{\lambda_{\ell'}}\right) e^{i\alpha}, \\
 \mathcal{E}_{\ell\ell'}^-(\mathbf{r}, \mathbf{r}'_{2b}) &= \mathcal{E}_{\ell\ell'}^-(\mathbf{r}, \mathbf{r}_c^{2b}) \sum_{n=0}^{\infty} \sum_{m=-n}^n 4\pi (-1)^{n+m} i_n(\lambda_{\ell'} r_s^{1b}) \overline{Y_n^m(\theta_s^{1b}, \varphi_s^{1b})} \widehat{P}_n^m\left(\frac{\lambda_{\ell'z}}{\lambda_{\ell'}}\right) e^{i\alpha},
 \end{aligned} \tag{3.20}$$

and

$$\begin{aligned}
 \mathcal{E}_{\ell\ell'}^+(\mathbf{r}, \mathbf{r}'_{1b}) &= \mathcal{E}_{\ell\ell'}^+(\mathbf{r}_c^t, \mathbf{r}'_{1b}) \sum_{n=0}^{\infty} \sum_{m=-n}^n 4\pi (-1)^n i_n(\lambda_{\ell} r_t) Y_n^m(\theta_t, \varphi_t) \widehat{P}_n^m\left(\frac{\lambda_{\ell z}}{\lambda_{\ell}}\right) e^{-i\alpha}, \\
 \mathcal{E}_{\ell\ell'}^-(\mathbf{r}, \mathbf{r}'_{2b}) &= \mathcal{E}_{\ell\ell'}^-(\mathbf{r}_c^t, \mathbf{r}'_{2b}) \sum_{n=0}^{\infty} \sum_{m=-n}^n 4\pi (-1)^m i_n(\lambda_{\ell} r_t) Y_n^m(\theta_t, \varphi_t) \widehat{P}_n^m\left(\frac{\lambda_{\ell z}}{\lambda_{\ell}}\right) e^{-i\alpha},
 \end{aligned} \tag{3.21}$$

for $b = 1, 2$. Then, a substitution of (3.20) into (2.14) gives the ME

$$\tilde{u}_{\ell\ell'}^{ab}(\mathbf{r}, \mathbf{r}'_{ab}) = \sum_{n=0}^{\infty} \sum_{m=-n}^n M_{nm}^{ab} \tilde{\mathcal{F}}_{nm}^{ab}(\mathbf{r}, \mathbf{r}_c^{ab}), \quad M_{nm}^{ab} = 4\pi i_n(\lambda_{\ell'} r_s^{ab}) \overline{Y_n^m(\theta_s^{ab}, \varphi_s^{ab})} \tag{3.22}$$

at equivalent polarization source centers \mathbf{r}_c^{ab} , and the LE

$$\tilde{u}_{\ell\ell'}^{ab}(\mathbf{r}, \mathbf{r}'_{ab}) = \sum_{n=0}^{\infty} \sum_{m=-n}^n L_{nm}^{ab} i_n(\lambda_{\ell} r_t) Y_n^m(\theta_t, \varphi_t) \tag{3.23}$$

at target center \mathbf{r}_c^t . Here, $\tilde{\mathcal{F}}_{nm}^{ab}(\mathbf{r}, \mathbf{r}_c^{ab})$ are represented by Sommerfeld-type integrals

$$\begin{aligned}
 \tilde{\mathcal{F}}_{nm}^{1b}(\mathbf{r}, \mathbf{r}_c^{1b}) &= \frac{1}{8\pi^2} \int_0^{\infty} \int_0^{2\pi} \frac{\lambda_{\rho}}{\lambda_{\ell z}} \mathcal{E}_{\ell\ell'}^+(\mathbf{r}, \mathbf{r}_c^{1b}) \sigma_{\ell\ell'}^{1b}(\lambda_{\rho}) \widehat{P}_n^m\left(\frac{\lambda_{\ell'z}}{\lambda_{\ell'}}\right) e^{i\alpha} d\alpha d\lambda_{\rho}, \\
 \tilde{\mathcal{F}}_{nm}^{2b}(\mathbf{r}, \mathbf{r}_c^{2b}) &= \frac{(-1)^{n+m}}{8\pi^2} \int_0^{\infty} \int_0^{2\pi} \frac{\lambda_{\rho}}{\lambda_{\ell z}} \mathcal{E}_{\ell\ell'}^-(\mathbf{r}, \mathbf{r}_c^{2b}) \sigma_{\ell\ell'}^{2b}(\lambda_{\rho}) \widehat{P}_n^m\left(\frac{\lambda_{\ell'z}}{\lambda_{\ell'}}\right) e^{i\alpha} d\alpha d\lambda_{\rho},
 \end{aligned} \tag{3.24}$$

and the LE coefficients are given by

$$\begin{aligned}
 I_{nm}^{1b} &= \frac{(-1)^n}{2\pi} \int_0^\infty \int_0^{2\pi} \frac{\lambda_\rho}{\lambda_{\ell z}} \mathcal{E}_{\ell\ell'}^+(\mathbf{r}_c^t, \mathbf{r}'_{1b}) \sigma_{\ell\ell'}^{1b}(\lambda_\rho) \widehat{P}_n^m\left(\frac{\lambda_{\ell z}}{\lambda_\ell}\right) e^{-im\alpha} d\alpha d\lambda_\rho, \\
 I_{nm}^{2b} &= \frac{(-1)^m}{2\pi} \int_0^\infty \int_0^{2\pi} \frac{\lambda_\rho}{\lambda_{\ell z}} \mathcal{E}_{\ell\ell'}^-(\mathbf{r}_c^t, \mathbf{r}'_{2b}) \sigma_{\ell\ell'}^{2b}(\lambda_\rho) \widehat{P}_n^m\left(\frac{\lambda_{\ell z}}{\lambda_\ell}\right) e^{-im\alpha} d\alpha d\lambda_\rho.
 \end{aligned}
 \tag{3.25}$$

According to the definition of $\mathcal{E}_{\ell\ell'}^-(\mathbf{r}, \mathbf{r}')$ and $\mathcal{E}_{\ell\ell'}^+(\mathbf{r}, \mathbf{r}')$ in (2.16), the centers \mathbf{r}_c^{ab} and \mathbf{r}_c^t must satisfy

$$z_c^{1b} < d_\ell, \quad z_c^{2b} > d_{\ell-1}, \tag{3.26}$$

and

$$z_c^t > d_\ell \text{ in FMM for } \tilde{u}_{\ell\ell'}^{1b}(\mathbf{r}, \mathbf{r}'_{1b}); \quad z_c^t < d_{\ell-1} \text{ in FMM for } \tilde{u}_{\ell\ell'}^{2b}(\mathbf{r}, \mathbf{r}'_{2b}), \tag{3.27}$$

respectively, to ensure the exponential decay in $\mathcal{E}_{\ell\ell'}^+(\mathbf{r}, \mathbf{r}_c^{1b})$, $\mathcal{E}_{\ell\ell'}^-(\mathbf{r}, \mathbf{r}_c^{2b})$ and $\mathcal{E}_{\ell\ell'}^+(\mathbf{r}_c^t, \mathbf{r}'_{1b})$, $\mathcal{E}_{\ell\ell'}^-(\mathbf{r}_c^t, \mathbf{r}'_{2b})$ as $\lambda_\rho \rightarrow \infty$ and hence the convergence of the corresponding Sommerfeld-type integrals in (3.24) and (3.25). These restrictions can be met in practice, since we are considering targets in the ℓ -th layer and the equivalent polarization coordinates are always located above the interface $z = d_{\ell-1}$ or below the interface $z = d_\ell$.

Next, we discuss the center shifting and translation for ME (3.22) and LE (3.23). A desirable feature of the expansions of reaction components discussed above is that the formula (3.22) for the ME coefficients and the formula (3.23) for the LE have exactly the same form as the formulas of ME coefficients and LE for free space Green's function. Therefore, we can see that center shifting for MEs and LEs are the same as free space case given in (3.5).

It suffices to derive the translation from ME (3.22) to LE (3.23). Recall the definition of exponential functions in (2.15), $\mathcal{E}_{\ell\ell'}^+(\mathbf{r}, \mathbf{r}_c^{1b})$ and $\mathcal{E}_{\ell\ell'}^-(\mathbf{r}, \mathbf{r}_c^{2b})$ have the following splitting

$$\begin{aligned}
 \mathcal{E}_{\ell\ell'}^+(\mathbf{r}, \mathbf{r}_c^{1b}) &= \mathcal{E}_{\ell\ell'}^+(\mathbf{r}_c^t, \mathbf{r}_c^{1b}) e^{i\lambda_\alpha \cdot (\rho - \rho_c^t)} e^{-\lambda_{\ell z} (z - z_c^t)}, \\
 \mathcal{E}_{\ell\ell'}^-(\mathbf{r}, \mathbf{r}_c^{2b}) &= \mathcal{E}_{\ell\ell'}^-(\mathbf{r}_c^t, \mathbf{r}_c^{2b}) e^{i\lambda_\alpha \cdot (\rho - \rho_c^t)} e^{\lambda_{\ell z} (z - z_c^t)}.
 \end{aligned}$$

Applying spherical harmonic expansion (3.16) again, we obtain

$$\begin{aligned}
 e^{i\lambda_\alpha \cdot (\rho - \rho_c^t) + \lambda_{\ell z} (z - z_c^t)} &= 4\pi \sum_{n=0}^\infty \sum_{m=-n}^n (-1)^m i_n(r_t) Y_n^m(\theta_t, \varphi_t) \widehat{P}_n^m\left(\frac{\lambda_{\ell z}}{\lambda_\ell}\right) e^{-im\alpha}, \\
 e^{i\lambda_\alpha \cdot (\rho - \rho_c^t) - \lambda_{\ell z} (z - z_c^t)} &= 4\pi \sum_{n=0}^\infty \sum_{m=-n}^n (-1)^n i_n(r_t) Y_n^m(\theta_t, \varphi_t) \widehat{P}_n^m\left(\frac{\lambda_{\ell z}}{\lambda_\ell}\right) e^{-im\alpha}.
 \end{aligned}$$

Substituting into (3.22), the ME is translated to the LE (3.23) via

$$I_{nm}^{1b} = \sum_{v=0}^\infty \sum_{|\mu|=0}^v T_{nm, v\mu}^{1b} M_{v\mu}^{1b}, \quad I_{nm}^{2b} = \sum_{v=0}^\infty \sum_{|\mu|=0}^v T_{nm, v\mu}^{2b} M_{v\mu}^{2b}, \tag{3.28}$$

and the M2L translation operators are given in integral forms as follows

$$\begin{aligned}
 T_{nm, v\mu}^{1b} &= \frac{(-1)^n}{2\pi} \int_0^\infty \int_0^{2\pi} \frac{\lambda_\rho}{\lambda_{\ell z}} \mathcal{E}^+(\mathbf{r}_c^t, \mathbf{r}_c^{1b}) \sigma_{\ell\ell'}^{1b}(\lambda_\rho) Q_{nm}^{v\mu}(\lambda_\rho) e^{i(\mu-m)\alpha} d\alpha d\lambda_\rho, \\
 T_{nm, v\mu}^{2b} &= \frac{(-1)^{m+v+\mu}}{2\pi} \int_0^\infty \int_0^{2\pi} \frac{\lambda_\rho}{\lambda_{\ell z}} \mathcal{E}^-(\mathbf{r}_c^t, \mathbf{r}_c^{2b}) \sigma_{\ell\ell'}^{2b}(\lambda_\rho) Q_{nm}^{v\mu}(\lambda_\rho) e^{i(\mu-m)\alpha} d\alpha d\lambda_\rho,
 \end{aligned}
 \tag{3.29}$$

where

$$Q_{nm}^{v\mu}(\lambda_\rho) = \widehat{P}_n^m\left(\frac{\lambda_{\ell z}}{\lambda_\ell}\right) \widehat{P}_v^\mu\left(\frac{\lambda_{\ell' z}}{\lambda_{\ell'}}\right).$$

Again, the convergence of the Sommerfeld-type integrals in (3.29) is ensured by the conditions in (3.26)-(3.27).

To end this subsection, we give some numerical examples to show the convergence behavior of the MEs in (3.22). Consider the MEs of $\tilde{u}_{11}^{11}(\mathbf{r}, \mathbf{r}'_{11})$ and $\tilde{u}_{11}^{22}(\mathbf{r}, \mathbf{r}'_{22})$ in a three-layer medium with $\varepsilon_0 = 1.0$, $\varepsilon_1 = 8.6$, $\varepsilon_2 = 20.5$, $\lambda_0 = 1.2$, $\lambda_1 = 0.5$, $\lambda_2 = 2.1$, $d_0 = 0$, $d_1 = -1.2$. In the following examples, we fix $\mathbf{r}' = (0.625, 0.5, -0.1)$ in the middle layer and use definition (2.13) which gives $\mathbf{r}'_{11} = (0.625, 0.5, -2.3)$, $\mathbf{r}'_{22} = (0.625, 0.5, 0.1)$. The centers for MEs are set to be $\mathbf{r}_c^{11} =$

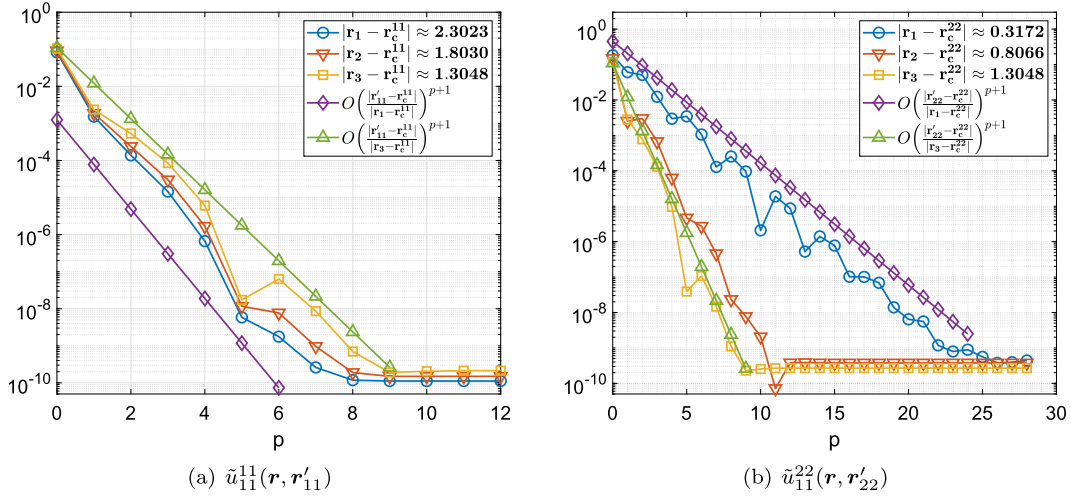


Fig. 3.2. Exponential convergence of the MEs for reaction components.

(0.6, 0.6, -2.4), $\mathbf{r}_c^{22} = (0.6, 0.6, 0.2)$, which implies $|\mathbf{r}'_{11} - \mathbf{r}_c^{11}| = |\mathbf{r}'_{22} - \mathbf{r}_c^{22}| \approx 0.1436$. For both components, we test three targets given by

$$\mathbf{r}_1 = (0.5, 0.625, -0.1), \quad \mathbf{r}_2 = (0.5, 0.625, -0.6), \quad \mathbf{r}_3 = (0.5, 0.625, -1.1).$$

The relative errors against truncation number p are depicted in Fig. 3.2. We also plot the convergence rates similar with that of the ME for free space Green's function, i.e., $O\left[\left(\frac{|\mathbf{r}-\mathbf{r}_c^{ab}|}{|\mathbf{r}'_{ab}-\mathbf{r}_c^{ab}|}\right)^{p+1}\right]$ as reference convergence rates. The results clearly show that ME of reaction components $u_{11}^1(\mathbf{r}, \mathbf{r}'_{11})$ and $u_{11}^2(\mathbf{r}, \mathbf{r}'_{22})$ have an exponential convergence rate $O\left[\left(\frac{|\mathbf{r}-\mathbf{r}_c^{ab}|}{|\mathbf{r}'_{ab}-\mathbf{r}_c^{ab}|}\right)^{p+1}\right]$ similar as that of free space Green's function. Therefore, the ME (3.22) can be used to develop FMM for efficient computation of the reaction components as in the Yukawa-FMM for the free space Green's function.

Remark 3.1. Although the derivation of ME (3.22) is based on the spherical harmonic expansion (3.16), the final expansion does take advantage of the specific symmetry of the layered media. In fact, the expansion basis functions (3.24) can be seen as a superposition of cylindrical Bessel functions, which have symmetry in the xy -plane. This fact is clear in the simplified expressions in (3.38). This symmetry is surely related to the special geometry of the layered media, i.e., cylindrical symmetry in the xy -plane.

Remark 3.2. The technique presented above can also be applied to the Green's function of the PB equation in free space. A remarkable fact is that it will give the classic theoretical results (3.1)–(3.4) which was derived from well-known addition theorem.

Actually, the Green's function of the linearized PB equation in free space has a Sommerfeld-type integral representation

$$k_0(\lambda|\mathbf{r}|) = \frac{\pi}{2} \frac{e^{-\lambda|\mathbf{r}|}}{\lambda|\mathbf{r}|} = \frac{1}{4\lambda} \int_0^\infty \int_0^{2\pi} \lambda_\rho e^{i\lambda_\rho(x\cos\alpha+y\sin\alpha)} \frac{e^{-\lambda_z|z|}}{\lambda_z} d\alpha d\lambda_\rho, \tag{3.30}$$

where $\lambda_z = \sqrt{\lambda^2 + \lambda_\rho^2}$. In the spectral domain, the source-target separation can be achieved straightforwardly as

$$\begin{aligned} k_0(\lambda|\mathbf{r}-\mathbf{r}'|) &= \frac{1}{4\lambda} \int_0^\infty \int_0^{2\pi} \lambda_\rho \frac{e^{\lambda\cdot(\mathbf{r}-\mathbf{r}'_c^s)} e^{-\lambda\cdot(\mathbf{r}'-\mathbf{r}'_c^s)}}{\lambda_z} d\alpha d\lambda_\rho, \\ k_0(\lambda|\mathbf{r}-\mathbf{r}'|) &= \frac{1}{4\lambda} \int_0^\infty \int_0^{2\pi} \lambda_\rho \frac{e^{\lambda\cdot(\mathbf{r}-\mathbf{r}'_c^t)} e^{-\lambda\cdot(\mathbf{r}'-\mathbf{r}'_c^t)}}{\lambda_z} d\alpha d\lambda_\rho, \end{aligned} \tag{3.31}$$

for $z \geq z'$, where $\boldsymbol{\lambda} = (i\lambda_\rho \cos\alpha, i\lambda_\rho \sin\alpha, -\lambda_z)$. Without loss of generality, here we only consider the case $z \geq z'$ for an illustration. Applying the spherical harmonic expansion (3.16) to exponential functions $e^{-\lambda\cdot(\mathbf{r}'-\mathbf{r}'_c^s)}$ and $e^{-\lambda\cdot(\mathbf{r}-\mathbf{r}'_c^t)}$ in (3.31) gives

$$k_0(\lambda|\mathbf{r} - \mathbf{r}'|) = \sum_{n=0}^{\infty} \sum_{m=-n}^n \frac{M_{nm}}{4\lambda} \int_0^{\infty} \int_0^{2\pi} \lambda \rho \frac{e^{\lambda \cdot (\mathbf{r} - \mathbf{r}'_c)}}{\lambda_z} \widehat{P}_n^m\left(\frac{\lambda_z}{\lambda}\right) e^{im\alpha} d\alpha d\lambda \rho, \quad (3.32)$$

and

$$k_0(\lambda|\mathbf{r} - \mathbf{r}'|) = \sum_{n=0}^{\infty} \sum_{m=-n}^n \widehat{L}_{nm} i_n(kr_t) Y_n^m(\theta_t, \phi_t), \quad (3.33)$$

for $z \geq z'$, where M_{nm} is defined in (3.3) and

$$\widehat{L}_{nm} = \frac{(-1)^n}{4\lambda} \int_0^{\infty} \int_0^{2\pi} \lambda \rho \frac{e^{\lambda \cdot (\mathbf{r}'_c - \mathbf{r}')}}{\lambda_z} \widehat{P}_n^m\left(\frac{\lambda_z}{\lambda}\right) e^{-im\alpha} d\alpha d\lambda \rho. \quad (3.34)$$

For the convergence of the Sommerfeld-type integrals in the above expansions, we only consider centers with properties $z_c^s < z$ and $z_c^t > z'$. Recalling the identity

$$k_n(\lambda|\mathbf{r}|) Y_n^m(\theta, \varphi) = \frac{1}{4\lambda} \int_0^{\infty} \int_0^{2\pi} \lambda \rho \frac{e^{\lambda \cdot \mathbf{r}}}{\lambda_z} \widehat{P}_n^m\left(\frac{\lambda_z}{\lambda}\right) e^{im\alpha} d\alpha d\lambda \rho \quad (3.35)$$

for $z \geq 0$, we see that (3.32) and (3.33) are exactly the multipole and local expansions (3.1)–(3.2) for the case of $z \geq z'$, respectively.

3.3. The FMM algorithm and efficient calculation of the Sommerfeld-type integrals

The framework of the traditional FMM together with ME (3.22), LE (3.23), M2L translation (3.28)–(3.29), and ME and LE center shifting (3.5) constitute the FMM for the computation of reaction components $\Phi_{\ell\ell'}^{ab}(\mathbf{r}_{\ell i})$, $a, b = 1, 2$. In the FMM for each reaction component, a large box is defined to include all equivalent polarization charge coordinates and corresponding target particles, where the adaptive tree structure will be built by a bisection procedure, see Fig. 2.4 (right). Note that the validity of the ME (3.22), LE (3.23), and M2L translation (3.28) used in the algorithm imposes restrictions (3.27) on the centers, accordingly. This can be ensured by setting the largest box for the specific reaction component to be equally divided by the interface between equivalent polarization coordinates and targets, see Fig. 2.4. Thus, the largest box for the FMM implementation will be different for different reaction components. With this setting, all source and target boxes of level higher than zeroth level in the adaptive tree structure will have centers below or above the interfaces, accordingly. The fast multipole algorithm for the computation of the reaction component $\Phi_{\ell\ell'}^{ab}(\mathbf{r}_{\ell i})$ is summarized in Algorithm 1. All the interactions given by (2.11) will be obtained by first calculating all components and then summing them up. Framework of the algorithm is presented in Algorithm 2.

The double integrals involved in the ME, LE and M2L translations can be simplified by using the following identity

$$J_n(z) = \frac{1}{2\pi i^n} \int_0^{2\pi} e^{iz \cos\theta + in\theta} d\theta. \quad (3.36)$$

With the definitions

$$\mathcal{Z}_{\ell\ell'}^+(z, z') := e^{-\lambda_{\ell z}(z-d_{\ell}) - \lambda_{\ell' z}(d_{\ell} - z')}, \quad \mathcal{Z}_{\ell\ell'}^-(z, z') := e^{-\lambda_{\ell z}(d_{\ell-1} - z) - \lambda_{\ell' z}(z' - d_{\ell-1})}, \quad (3.37)$$

the ME functions in (3.24) can be simplified as

$$\begin{aligned} \widetilde{\mathcal{F}}_{nm}^{1b}(\mathbf{r}, \mathbf{r}_c^{1b}) &= \frac{e^{im\varphi_s^{1b}}}{4\pi} \int_0^{\infty} \lambda \rho J_m(\lambda \rho \rho_s^{1b}) \frac{\mathcal{Z}_{\ell\ell'}^+(z, z_c^{1b})}{\lambda_{\ell z}} \sigma_{\ell\ell'}^{1b}(\lambda \rho) i^m \widehat{P}_n^m\left(\frac{\lambda_{\ell' z}}{\lambda_{\ell' z}}\right) d\lambda \rho, \\ \widetilde{\mathcal{F}}_{nm}^{2b}(\mathbf{r}, \mathbf{r}_c^{2b}) &= \frac{(-1)^{n+m} e^{im\varphi_s^{2b}}}{4\pi} \int_0^{\infty} \lambda \rho J_m(\lambda \rho \rho_s^{2b}) \frac{\mathcal{Z}_{\ell\ell'}^-(z, z_c^{2b})}{\lambda_{\ell z}} \sigma_{\ell\ell'}^{2b}(\lambda \rho) i^m \widehat{P}_n^m\left(\frac{\lambda_{\ell' z}}{\lambda_{\ell' z}}\right) d\lambda \rho, \end{aligned} \quad (3.38)$$

and the expression (3.25) for LE coefficients can be simplified as

Algorithm 1 FMM for general reaction component $\Phi_{\ell\ell'}^{\text{ab}}(\mathbf{r}_{\ell i}), i = 1, 2, \dots, N_{\ell}$.

```

Determine z-coordinates of equivalent polarization sources for all source particles.
Generate an adaptive hierarchical tree structure with polarization sources  $\{Q_{\ell'j}, \mathbf{r}_{\ell'j}^{\text{ab}}\}_{j=1}^{N_{\ell'}}$  and targets  $\{\mathbf{r}_{\ell i}\}_{i=1}^{N_{\ell}}$ .
Upward pass:
for  $l = H \rightarrow 0$  do
  for all boxes  $j$  on source tree level  $l$  do
    if  $j$  is a leaf node then
      form the free-space ME using Eq. (3.22).
    else
      form the free-space ME by merging children's expansions using the free-space center shift translation operator (3.5).
    end if
  end for
end for
Downward pass:
for  $l = 1 \rightarrow H$  do
  for all boxes  $j$  on target tree level  $l$  do
    shift the LE of  $j$ 's parent to  $j$  itself using the free-space shifting (3.5).
    collect interaction list contribution using the source box to target box translation operator in Eq. (3.28) while  $T_{nm,v\mu}^{\text{ab}}$  are computed using (3.41), (3.46) and forward recursion (3.48) for  $S_{nm,ij}^{\text{ab}}$ .
  end for
end for
Evaluate LEs:
for each leaf node (childless box) do
  evaluate the LE at each particle location.
end for
Local Direct Interactions:
for  $i = 1 \rightarrow N$  do
  compute Eq. (2.18) of target particle  $i$  in the neighboring boxes using DE quadrature for  $I_{00}^{\text{ab}}(\rho, z, z')$ .
end for

```

$$I_{nm}^{1b} = (-1)^n e^{-im\varphi_t^{1b}} \int_0^{\infty} \lambda_{\rho} J_{-m}(\lambda_{\rho} \rho_t^{1b}) \frac{Z_{\ell\ell'}^+(z_c^t, z_{1b}^t)}{\lambda_{\ell z}} \sigma_{\ell\ell'}^{1b}(\lambda_{\rho}) i^{-m} \widehat{P}_n^m\left(\frac{\lambda_{\ell z}}{\lambda_{\ell}}\right) d\lambda_{\rho},$$

$$I_{nm}^{2b} = (-1)^m e^{-im\varphi_t^{2b}} \int_0^{\infty} \lambda_{\rho} J_{-m}(\lambda_{\rho} \rho_t^{2b}) \frac{Z_{\ell\ell'}^-(z_c^t, z_{2b}^t)}{\lambda_{\ell z}} \sigma_{\ell\ell'}^{2b}(\lambda_{\rho}) i^{-m} \widehat{P}_n^m\left(\frac{\lambda_{\ell z}}{\lambda_{\ell}}\right) d\lambda_{\rho},$$

for $b = 1, 2$, where $(\rho_s^{\text{ab}}, \varphi_s^{\text{ab}})$ and $(\rho_t^{\text{ab}}, \varphi_t^{\text{ab}})$ are polar coordinates of $\mathbf{r} - \mathbf{r}_c^{\text{ab}}$ and $\mathbf{r}_c^t - \mathbf{r}_{\text{ab}}^t$ projected onto xy plane. Moreover, the M2L translation (3.29) can be simplified as

$$T_{nm,v\mu}^{1b} = (-1)^n D_{m\mu}^{(1)}(\varphi_{st}^{1b}) \int_0^{\infty} \lambda_{\rho} J_{\mu-m}(\lambda_{\rho} \rho_{st}^{1b}) \frac{Z_{\ell\ell'}^+(z_c^t, z_c^{1b})}{\lambda_{\ell z}} Q_{nm}^{v\mu}(\lambda_{\rho}) \sigma_{\ell\ell'}^{1b}(\lambda_{\rho}) d\lambda_{\rho},$$

$$T_{nm,v\mu}^{2b} = (-1)^v D_{m\mu}^{(2)}(\varphi_{st}^{2b}) \int_0^{\infty} \lambda_{\rho} J_{\mu-m}(\lambda_{\rho} \rho_{st}^{2b}) \frac{Z_{\ell\ell'}^-(z_c^t, z_c^{2b})}{\lambda_{\ell z}} Q_{nm}^{v\mu}(\lambda_{\rho}) \sigma_{\ell\ell'}^{2b}(\lambda_{\rho}) d\lambda_{\rho},$$
(3.39)

where $(\rho_{st}^{\text{ab}}, \varphi_{st}^{\text{ab}})$ is the polar coordinates of $\mathbf{r}_c - \mathbf{r}_c^{\text{ab}}$ projected in xy plane, respectively, and

$$D_{m\mu}^{(1)}(\varphi) = i^{\mu-m} e^{i(\mu-m)\varphi}, \quad D_{m\mu}^{(2)}(\varphi) = (-1)^{m+\mu} i^{\mu-m} e^{i(\mu-m)\varphi}.$$

Next, defining integrals

$$I_{nm,v\mu}^{1b}(\rho, z, z') = \int_0^{\infty} \lambda_{\rho} J_{\mu-m}(\lambda_{\rho} \rho) \frac{Z_{\ell\ell'}^+(z, z') \sigma_{\ell\ell'}^{1b}(\lambda_{\rho})}{\lambda_{\ell z}} i^{\mu-m} Q_{nm}^{v\mu}(\lambda_{\rho}) d\lambda_{\rho},$$

$$I_{nm,v\mu}^{2b}(\rho, z, z') = \int_0^{\infty} \lambda_{\rho} J_{\mu-m}(\lambda_{\rho} \rho) \frac{Z_{\ell\ell'}^-(z, z') \sigma_{\ell\ell'}^{2b}(\lambda_{\rho})}{\lambda_{\ell z}} i^{\mu-m} Q_{nm}^{v\mu}(\lambda_{\rho}) d\lambda_{\rho},$$
(3.40)

we have

Algorithm 2 3-D FMM for (2.11).

```

for  $\ell = 0 \rightarrow L$  do
  use classic FMM-Yukawa algorithm to compute  $\Phi_\ell^{free}(\mathbf{r}_{\ell i}), i = 1, 2, \dots, N_\ell$ .
end for
for  $\ell = 0 \rightarrow L - 1$  do
  for  $\ell' = 0 \rightarrow L - 1$  do
    use Algorithm 1 to compute  $\Phi_{\ell\ell'}^{11}(\mathbf{r}_{\ell i}), i = 1, 2, \dots, N_\ell$ .
  end for
  for  $\ell' = 1 \rightarrow L$  do
    use Algorithm 1 to compute  $\Phi_{\ell\ell'}^{12}(\mathbf{r}_{\ell i}), i = 1, 2, \dots, N_\ell$ .
  end for
end for
for  $\ell = 1 \rightarrow L$  do
  for  $\ell' = 0 \rightarrow L - 1$  do
    use Algorithm 1 to compute  $\Phi_{\ell\ell'}^{21}(\mathbf{r}_{\ell i}), i = 1, 2, \dots, N_\ell$ .
  end for
  for  $\ell' = 1 \rightarrow L$  do
    use Algorithm 1 to compute  $\Phi_{\ell\ell'}^{22}(\mathbf{r}_{\ell i}), i = 1, 2, \dots, N_\ell$ .
  end for
end for
    
```

$$\begin{aligned}
 \tilde{\mathcal{F}}_{nm}^{1b}(\mathbf{r}, \mathbf{r}_c^{1b}) &= \frac{e^{im\varphi_s^{1b}}}{\sqrt{4\pi}} I_{00, nm}^{1b}(\rho_s^{1b}, z, z_c^{1b}), & \tilde{\mathcal{F}}_{nm}^{2b}(\mathbf{r}, \mathbf{r}_c^{2b}) &= \frac{(-1)^{n+m} e^{im\varphi_s^{2b}}}{\sqrt{4\pi}} I_{00, nm}^{2b}(\rho_s^{2b}, z, z_c^{2b}), \\
 L_{nm}^{1b} &= (-1)^n \sqrt{4\pi} e^{-im\varphi_t^{1b}} I_{nm, 00}^{1b}(\rho_t^{1b}, z_t^t, z_{1b}^t), & L_{nm}^{2b} &= (-1)^m \sqrt{4\pi} e^{-im\varphi_t^{2b}} I_{nm, 00}^{2b}(\rho_t^{2b}, z_{2b}^t, z_c^t), \\
 T_{nm, \nu\mu}^{1b} &= (-1)^n e^{i(\mu-m)\varphi_{st}^{1b}} I_{nm, \nu\mu}^{1b}(\rho_{st}^{1b}, z_t^t, z_c^{1b}), & T_{nm, \nu\mu}^{2b} &= (-1)^{\nu+m+\mu} e^{i(\mu-m)\varphi_{st}^{2b}} I_{nm, \nu\mu}^{2b}(\rho_{st}^{2b}, z_t^t, z_c^{2b}).
 \end{aligned}
 \tag{3.41}$$

The FMM demands efficient computation of the Sommerfeld-type integrals $I_{nm, \nu\mu}^{ab}$ defined in (3.40). These integrals are convergent when the target and source particles are not exactly on the interfaces of a layered medium. High order quadrature rules could be used for direct numerical computation at runtime. However, this becomes prohibitively expensive due to a large number of integrals needed in the FMM. In fact, $O(p^4)$ integrals are required for each source box to target box translation, where p is the truncation index of the ME in the algorithm. Moreover, the involved integrand decays more slowly as the order of the involved associated Legendre function increases.

The Sommerfeld-type integrals $I_{nm, \nu\mu}^{ab}$ involves $Q_{nm}^{\nu\mu}(\lambda_\rho)$, the product of two associated Legendre functions. This term can be simplified by expressing its polynomial part into Legendre polynomials. Define

$$c_{nm} = \sqrt{\frac{2n+1}{4\pi} \frac{(n-m)!}{(n+m)!}}, \quad a_{nm}^j = \frac{(-1)^{n-j} (2j)! c_{nm}}{2^n j! (n-j)! (2j-n-m)!},
 \tag{3.42}$$

and

$$b_{nm}^s = \sum_{j=q}^n \frac{(-1)^s a_{nm}^j (j-r)!}{s! (j-r-s)!}, \quad q = \max\left(\left\lceil \frac{n+m}{2} \right\rceil, s+r\right).
 \tag{3.43}$$

The derivation in [1] gives

$$\hat{P}_n^m\left(\frac{\lambda_{\ell z}}{\lambda_\ell}\right) \hat{P}_\nu^\mu\left(\frac{\lambda_{\ell' z}}{\lambda_{\ell'}}\right) = \sum_{s=0}^{n-r+\nu-r'} C_{n\nu m\mu}^s \lambda_\rho^{|m|+|\mu|+2s} \left(\frac{\lambda_\ell}{\lambda_{\ell z}}\right)^i \left(\frac{\lambda_{\ell'}}{\lambda_{\ell' z}}\right)^j
 \tag{3.44}$$

for all $n, \nu = 0, 1, \dots$, and $-n \leq m \leq n, -\nu \leq \mu \leq \nu$, where $i = (n + |m|) \pmod{2}, j = (\nu + |\mu|) \pmod{2}, r = \lfloor (n + |m|)/2 \rfloor, r' = \lfloor (\nu + |\mu|)/2 \rfloor$, and

$$C_{n\nu m\mu}^s = \sum_{t=\max(s-\nu+r', 0)}^{\min(s, n-r)} \frac{\tau_m \tau_\nu b_{n|m|}^t b_{\nu|\mu|}^{s-t} (|m| + |\mu| + 2s)!}{(i\lambda_\ell)^{|m|+2t} (i\lambda_{\ell'})^{|\mu|+2(s-t)}}, \quad \tau_\nu = \begin{cases} 1, & \nu \geq 0, \\ (-1)^{-\nu}, & \nu < 0. \end{cases}$$

Defining integrals

$$\begin{aligned}
 S_{nm, ij}^{1b}(\rho, z, z') &= \int_0^\infty \frac{\lambda_\rho^n J_m(\lambda_\rho \rho) \mathcal{Z}_{\ell\ell'}^+(z, z')}{\sqrt{(n+m)!(n-m)!}} \frac{\sigma_{\ell\ell'}^{1b}(\lambda_\rho)}{\lambda_{\ell z}} \left(\frac{\lambda_\ell}{\lambda_{\ell z}}\right)^i \left(\frac{\lambda_{\ell'}}{\lambda_{\ell' z}}\right)^j d\lambda_\rho, \\
 S_{nm, ij}^{2b}(\rho, z, z') &= \int_0^\infty \frac{\lambda_\rho^n J_m(\lambda_\rho \rho) \mathcal{Z}_{\ell\ell'}^-(z, z')}{\sqrt{(n+m)!(n-m)!}} \frac{\sigma_{\ell\ell'}^{2b}(\lambda_\rho)}{\lambda_{\ell z}} \left(\frac{\lambda_\ell}{\lambda_{\ell z}}\right)^i \left(\frac{\lambda_{\ell'}}{\lambda_{\ell' z}}\right)^j d\lambda_\rho,
 \end{aligned}
 \tag{3.45}$$

for $i, j = 0, 1$, we have

$$I_{nm,v\mu}^{ab}(\rho, z, z') = i^{\mu-m} \sum_{s=0}^{n-r+v-r'} \tilde{C}_{nvm\mu}^s S_{|m|+|\mu|+2s+1,\mu-m,ij}^{ab}(\rho, z, z'), \tag{3.46}$$

where

$$\tilde{C}_{nvm\mu}^s = \sqrt{(|m| - m + |\mu| + \mu + 2s + 1)(|m| + m + |\mu| - \mu + 2s + 1)} C_{nvm\mu}^s.$$

Another important technical aspect in the implementation of the FMM involves scaling. Since $M_{nm}^{ab} \approx (|\mathbf{r} - \mathbf{r}_c^{ab}|)^n, L_{nm}^{ab} \approx (|\mathbf{r}^{ab} - \mathbf{r}_c^t|)^{-n}$, a naive use of the expansions (3.22) and (3.23) in the implementation of FMM is likely to encounter underflow and overflow issues. To avoid this, one need to scale various expansions, replacing M_{nm}^{ab} by M_{nm}^{ab}/S^n and L_{nm}^{ab} by $L_{nm}^{ab} \cdot S^n$ where S is the scaling factor. To compensate for this scaling, we replace $\tilde{\mathcal{F}}_{nm}^{ab}(\mathbf{r}, \mathbf{r}_c^{ab})$ with $\tilde{\mathcal{F}}_{nm}^{ab}(\mathbf{r}, \mathbf{r}_c^{ab}) \cdot S^n, T_{nm,n'm'}^{ab}$ with $T_{nm,n'm'}^{ab} \cdot S^{n+n'}$. Usually, the scaling factor S is chosen to be the size of the box in which the computation occurs. Therefore, the following scaled Sommerfeld-type integrals

$$\begin{aligned} S^n S_{nm,ij}^{1b}(\rho, z, z') &= S^n \int_0^\infty \frac{\lambda_\rho^n J_m(\lambda_\rho \rho) \mathcal{Z}_{\ell\ell'}^+(z, z')}{\sqrt{(n+m)!(n-m)!}} \frac{\sigma_{\ell\ell'}^{1b}(\lambda_\rho)}{\lambda_{\ell z}} \left(\frac{\lambda_\ell}{\lambda_{\ell z}}\right)^i \left(\frac{\lambda_{\ell'}}{\lambda_{\ell' z}}\right)^j d\lambda_\rho, \\ S^n S_{nm,ij}^{2b}(\rho, z, z') &= S^n \int_0^\infty \frac{\lambda_\rho^n J_m(\lambda_\rho \rho) \mathcal{Z}_{\ell\ell'}^-(z, z')}{\sqrt{(n+m)!(n-m)!}} \frac{\sigma_{\ell\ell'}^{2b}(\lambda_\rho)}{\lambda_{\ell z}} \left(\frac{\lambda_\ell}{\lambda_{\ell z}}\right)^i \left(\frac{\lambda_{\ell'}}{\lambda_{\ell' z}}\right)^j d\lambda_\rho, \end{aligned} \tag{3.47}$$

for all $n \geq m \geq 0$ are computed in the implementation. Recalling the recurrence formula

$$J_{m+1}(z) = \frac{2m}{z} J_m(z) - J_{m-1}(z),$$

and defining $a_n = \sqrt{n(n+1)}$, we have

$$\begin{aligned} S^n S_{nm+1,ij}^{ab}(\rho, z, z') &= \int_0^\infty \frac{(\lambda_\rho S)^n J_{m+1}(\lambda_\rho \rho) \mathcal{Z}_{\ell\ell'}^\pm(z, z')}{\sqrt{(n+m+1)!(n-m-1)!}} \frac{\sigma_{\ell\ell'}^{ab}(\lambda_\rho)}{\lambda_{\ell z}} \left(\frac{\lambda_\ell}{\lambda_{\ell z}}\right)^i \left(\frac{\lambda_{\ell'}}{\lambda_{\ell' z}}\right)^j d\lambda_\rho \\ &= \frac{2mS}{a_{n+m}\rho} \int_0^\infty \frac{(\lambda_\rho S)^{n-1} J_m(\lambda_\rho \rho) \mathcal{Z}_{\ell\ell'}^\pm(z, z')}{\sqrt{(n+m-1)!(n-m-1)!}} \frac{\sigma_{\ell\ell'}^{ab}(\lambda_\rho)}{\lambda_{\ell z}} \left(\frac{\lambda_\ell}{\lambda_{\ell z}}\right)^i \left(\frac{\lambda_{\ell'}}{\lambda_{\ell' z}}\right)^j d\lambda_\rho \\ &\quad - \frac{a_{n-m}}{a_{n+m}} \int_0^\infty \frac{(\lambda_\rho S)^n J_{m-1}(\lambda_\rho \rho) \mathcal{Z}_{\ell\ell'}^\pm(z, z')}{\sqrt{(n+m-1)!(n-m+1)!}} \frac{\sigma_{\ell\ell'}^{ab}(\lambda_\rho)}{\lambda_{\ell z}} \left(\frac{\lambda_\ell}{\lambda_{\ell z}}\right)^i \left(\frac{\lambda_{\ell'}}{\lambda_{\ell' z}}\right)^j d\lambda_\rho, \end{aligned}$$

which directly gives the following forward recurrence formula

$$S^n S_{nm+1,ij}^{ab} = \frac{2m}{a_{n+m}} \frac{S}{\rho} S^{n-1} S_{n-1,m,ij}^{ab} - \frac{a_{n-m}}{a_{n+m}} S^n S_{nm-1,ij}^{ab}, \quad n \geq m \geq 1. \tag{3.48}$$

We adopt the forward recurrence when

$$\frac{2m}{a_{n+m}} \frac{S}{\rho} < 1, \tag{3.49}$$

or equivalently

$$n > 2\sqrt{\frac{m^2 S^2}{\rho^2} + 1} - m - \frac{1}{2}. \tag{3.50}$$

Otherwise, the backward recursion

$$S^{n-1} S_{n-1,m,ij}^{ab} = \frac{a_{n+m}}{2m} \frac{\rho}{S} S^n S_{nm+1,ij}^{ab} + \frac{a_{n-m}}{2m} \frac{\rho}{S} S^n S_{nm-1,ij}^{ab} \tag{3.51}$$

will be adopted instead.

Let us first consider the computation of the integrals involved in the M2L translation matrices $T_{nm,n'm'}^{ab}$. For any polarization source box in the interaction list of a given target box, one will see that ρ_{ts}^{ab} is either 0 or larger than the box size S . If $\rho_{ts}^{ab} = 0$, we directly have

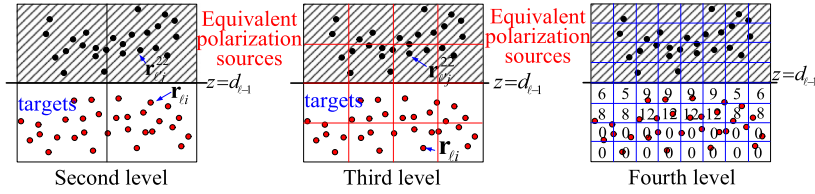


Fig. 3.3. Boxes in the source (shaded) and target tree for the computation of $\Phi_{\ell\ell'}^{22}(\mathbf{r}_{\ell i})$.

$$S^n S_{nm,ij}^{ab}(0, z, z') = 0, \quad \forall n \geq m > 0 \tag{3.52}$$

for any z and z' so the integrals are convergent. In all other cases, we have $\rho_{ts}^{ab} \geq S$ and the forward recurrence formula (3.48) is always used as we have

$$\frac{2m}{\sqrt{(n+m+1)(n+m)}} < \frac{1}{\sqrt{3}} < \frac{\rho_{ts}^{ab}}{S}, \quad n \geq m+1, \quad m \geq 1.$$

If the distribution of particles in the problem is not uniform, adaptive tree structure is usually used in the implementation of the FMM for a better performance. In these adaptive versions, computation of LE coefficients and potential directly using (3.25) and ME (3.22) will be performed if some conditions are satisfied (cf. [33]). In the computation of $\tilde{\mathcal{F}}_{nm}^{ab}(\mathbf{r}, \mathbf{r}_c^{ab}) \cdot S^n$ and $L_{nm}^{ab} \cdot S^n$, ρ_s^{ab} and ρ_t^{ab} could be arbitrarily small. Therefore, the backward recurrence formula (3.51) is required. Nevertheless, these direct computations are rarely used even in the FMM with an adaptive tree structure.

Given a truncation number p , the initial values $\{S_{n0,ij}^{ab}(\rho, z, z')\}_{n=0}^{2p+3}$ and $\{S_{n1,ij}^{ab}(\rho, z, z')\}_{n=1}^{2p+3}$ for the forward recursion (3.48) or the initial values $\{S_{(2p+3)m,ij}^{ab}(\rho, z, z')\}_{m=0}^{2p+3}$ for the backward recursion (3.51) are computed by using the DE quadrature (cf. [34,35]) rule along the positive real axis for $\rho \leq z + z'$. As in [2], the contour are changed to the positive imaginary axis when $\rho > z + z'$.

Remark 3.3. In the computation of a general reaction component $\Phi_{\ell\ell'}^{ab}(\mathbf{r}_{\ell i})$, $i = 1, 2, \dots, N_\ell$, the targets and equivalent polarization sources will locate at different sides of the material interface $z = d_{\ell-1}$ (if $a = 1$) or $z = d_\ell$ (if $a = 2$). Therefore, most, if not all, target boxes on the leaves of the target tree are far away from all source boxes on the leaves of the source tree. Usually, no direct interactions between sources and targets are calculated once the size of the smallest box is smaller than the minimum distance between sources and the corresponding interface. That means the time consuming computation of integrals $I_{00}^{ab}(\rho, z)$ for direct interaction is rarely performed in the FMM for reaction components. By the same reason, the interaction list of most target boxes in the target tree are empty. Therefore, the number of M2L translations in the FMM for reaction components are much less than that in the normal FMM for free space problems. To make it clear, we give an illustration in Fig. 3.3 using a 2-D tree structure for reaction component $\Phi_{\ell\ell'}^{22}(\mathbf{r}_{\ell i})$. The number of sources boxes in the interaction list of all target boxes in the fourth level of the target tree are counted (see the numbers in the 3rd subplot in Fig. 3.3). The discussions above explain the fact that the FMMs for reaction components are much more efficient than FMM for free space components when the number of sources and targets is large enough.

4. Numerical results

In this section, we present numerical results to demonstrate the performance of the proposed FMM for linearized Poisson-Boltzmann equation in layered media. This algorithm is implemented based on an open-source adaptive FMM package DASHMM [33] on a workstation with two Xeon E5-2699 v4 2.2 GHz processors (each has 22 cores) and 500 GB RAM using the GNU GCC compiler version 6.3.

We test the problem in a three-layer medium with interfaces placed at $z_0 = 0$, $z_1 = -1.2$. Particles are set to be uniformly distributed in irregular regions which are obtained by shifting the domain determined by $r = 0.5 - a + \frac{a}{8}(35 \cos^4 \theta - 30 \cos^2 \theta + 3)$ with $a = 0.1, 0.15, 0.05$ to new centers $(0, 0, 0.6)$, $(0, 0, -0.6)$ and $(0, 0, -1.8)$, respectively (see Fig. 4.1(a) for the cross section of the regions). All particles are generated by keeping the uniform distributed particles in a larger cube within the corresponding irregular regions. In the layered medium, the dielectric constants $\{\varepsilon_\ell\}_{\ell=0}^2$ and the inverse Debye-Huckel lengths $\{\lambda_\ell\}_{\ell=0}^2$ are set to be

$$\varepsilon_0 = 1.0, \quad \varepsilon_1 = 8.6, \quad \varepsilon_2 = 20.5, \quad \lambda_0 = 1.2, \quad \lambda_1 = 0.5, \quad \lambda_2 = 2.1.$$

Let $\tilde{\Phi}_\ell(\mathbf{r}_{\ell i})$ be the approximated values of $\Phi_\ell(\mathbf{r}_{\ell i})$ calculated by the proposed FMM. Define ℓ^2 and maximum errors as

$$Err_2^\ell := \sqrt{\frac{\sum_{i=1}^{N_\ell} |\Phi_\ell(\mathbf{r}_{\ell i}) - \tilde{\Phi}_\ell(\mathbf{r}_{\ell i})|^2}{\sum_{i=1}^{N_\ell} |\Phi_\ell(\mathbf{r}_{\ell i})|^2}}, \quad Err_{max}^\ell := \max_{1 \leq i \leq N_\ell} \frac{|\Phi_\ell(\mathbf{r}_{\ell i}) - \tilde{\Phi}_\ell(\mathbf{r}_{\ell i})|}{|\Phi_\ell(\mathbf{r}_{\ell i})|}. \tag{4.1}$$

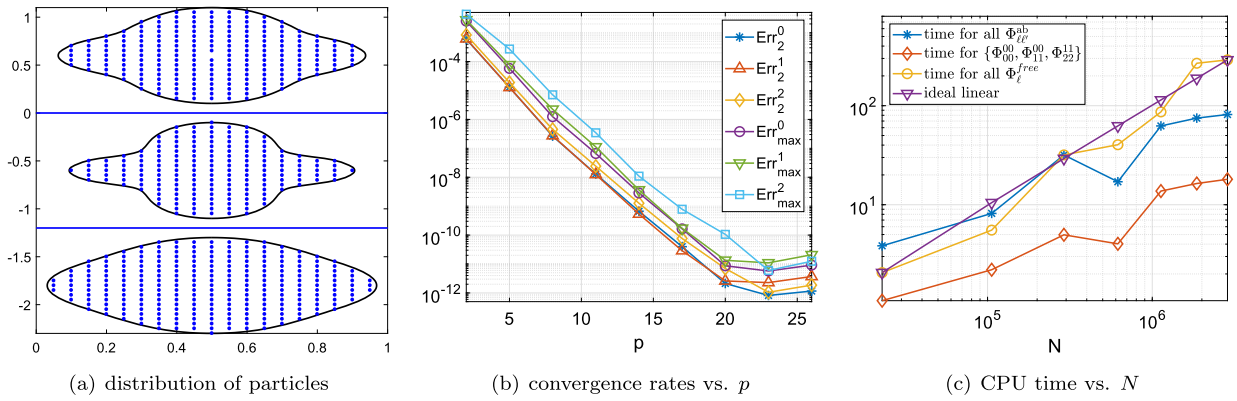


Fig. 4.1. Performance of FMM for a three layers media problem.

Table 4.1
Comparison of CPU time with multiple cores ($p = 5$).

Cores	N	Time for all $\{\Phi_{\ell}^{free}\}_{\ell=0}^2$	Time for all $\{\Phi_{\ell\ell'}^{a,b}\}$
1	618256	40.36	17.06
	1128556	86.72	62.47
	1862568	269.05	74.93
	2861288	292.42	81.47
6	618256	7.653	3.613
	1128556	16.29	12.50
	1862568	50.72	15.52
	2861288	54.85	17.27
36	618256	2.042	1.639
	1128556	4.308	4.459
	1862568	14.94	6.104
	2861288	15.21	7.673

For an accuracy test, we first consider $N = 912 + 640 + 1296$ particles in the irregular domains in three layers see Fig. 4.1 (a). Convergence rates against p are depicted in Fig. 4.1(b). Next, we test the FMM for up to 3 millions particles, and the CPU time for the computation of all three free space components $\{\Phi_{\ell}^{free}(\mathbf{r}_{\ell i})\}_{\ell=0}^2$, three selected reaction components $\{\Phi_{00}^{11}, \Phi_{11}^{11}, \Phi_{22}^{22}\}$ and all sixteen reaction components $\Phi_{\ell\ell'}^{a,b}(\mathbf{r}_{\ell i})$ with truncation $p = 5$ are compared in Fig. 4.1(c). It shows that all of them have an $O(N)$ complexity while the CPU time for the computation of reaction components has a much smaller linear scaling constant due to the fact that most of the equivalent polarization sources are well-separated from the targets. CPU time with multiple cores is given in Table 4.1 and it shows that, due to the small amount of CPU time in computing the reaction components, the speedup of the parallel computing is mainly decided by the computation of the free space components. Here, we only use parallel implementation within the computation of each component. Note the computation of each component is independent of others, so it is straightforward to implement a version of the code, which computes all components in parallel.

5. Conclusion

In this paper, we have presented a fast multipole method for charge interactions under the Poisson–Boltzmann potential in a 3-D layered electrolyte-dielectric media. The electrostatic potential of interest has been decomposed into a free space and four types of reaction field components. By extending the Funk-Hecke formula to pure imaginary wave numbers, we are able to develop the ME of $O(p^2)$ terms for the far field of the reaction components, which are associated with polarization sources at specific locations for each type of the reaction field components. M2L translation operators are also developed for the reaction components. As a result, the traditional FMM framework can be applied to both the free space and reaction components once the polarization sources are used together with the original targets. Due to the separation of the polarization sources and the corresponding target positions by a material interface, the computational cost for the reaction component is only a fraction of that of the FMM for the free space component. Hence, computing the potential in layered media basically costs the same as that for the electrostatic interactions in the free space.

For the future work, we will carry out error estimate of the FMM for the linearized Poisson–Boltzmann potential in 3-D layered media, which will require an error analysis for the MEs and M2L operators for the reaction components. The combination of the FMM with integral method for efficient simulation of ion channel transport in hybrid models as discussed in Section 2 will be naturally our next research work.

CRedit authorship contribution statement

All authors contributed equally to Conceptualization, Methodology, Software, Writing – original draft, Writing – review & editing.

Declaration of competing interest

The authors declare that they have no known competing financial interests or personal relationships that could have appeared to influence the work reported in this paper.

Acknowledgement

The first author acknowledges the financial support provided by NSFC (grant 11771137, 12022104) and the Construct Program of the Key Discipline in Hunan Province. This work was supported by US Army Research Office (Grant No. W911NF-17-1-0368) and US National Science Foundation (Grant No. DMS-1950471).

Appendix A. Reaction densities for a three layers medium

For a three layers medium with material parameters $\{\varepsilon_\ell, \lambda_\ell\}_{\ell=0}^2$, the expressions for the reaction densities are given as follows.

- Source in the top layer:

$$\begin{aligned} \sigma_{00}^{11}(\lambda_\rho) &= \frac{(\varepsilon_0\lambda_{0z} - \varepsilon_1\lambda_{1z})(\varepsilon_1\lambda_{1z} + \varepsilon_2\lambda_{2z}) + (\varepsilon_0\lambda_{0z} + \varepsilon_1\lambda_{1z})(\varepsilon_1\lambda_{1z} - \varepsilon_2\lambda_{2z})e^{2d_1\lambda_{1z}}}{2\varepsilon_0\kappa(\lambda_\rho)}, \\ \sigma_{10}^{11}(\lambda_\rho) &= \frac{\varepsilon_0\lambda_{1z}(\lambda_1\lambda_{1z} - \varepsilon_2\lambda_{2z})e^{d_1\lambda_{1z}}}{\varepsilon_0\kappa(\lambda_\rho)}, \quad \sigma_{10}^{21}(\lambda_\rho) = \frac{\varepsilon_0\lambda_{1z}(\varepsilon_1\lambda_{1z} + \varepsilon_2\lambda_{2z})}{\varepsilon_0\kappa(\lambda_\rho)}, \\ \sigma_{20}^{21}(\lambda_\rho) &= \frac{2\varepsilon_0\varepsilon_1\lambda_{1z}\lambda_{2z}e^{d_1\lambda_{1z}}}{\varepsilon_0\kappa(\lambda_\rho)}. \end{aligned}$$

- Source in the middle layer:

$$\begin{aligned} \sigma_{01}^{11}(\lambda_\rho) &= \frac{\varepsilon_1\lambda_{0z}(\varepsilon_1\lambda_{1z} - \varepsilon_2\lambda_{2z})e^{d_1\lambda_{1z}}}{\varepsilon_1\kappa(\lambda_\rho)}, \quad \sigma_{01}^{12}(\lambda_\rho) = \frac{\varepsilon_1\lambda_{0z}(\varepsilon_1\lambda_{1z} + \varepsilon_2\lambda_{2z})}{\varepsilon_1\kappa(\lambda_\rho)}, \\ \sigma_{11}^{11}(\lambda_\rho) &= \frac{(\varepsilon_1\lambda_{1z} - \varepsilon_2\lambda_{2z})(\varepsilon_1\lambda_{1z} + \varepsilon_0\lambda_{0z})}{2\varepsilon_1\kappa(\lambda_\rho)}, \\ \sigma_{11}^{12}(\lambda_\rho) &= \frac{(\varepsilon_1\lambda_{1z} - \varepsilon_2\lambda_{2z})(\varepsilon_1\lambda_{1z} - \varepsilon_0\lambda_{0z})e^{d_1\lambda_{1z}}}{2\varepsilon_1\kappa(\lambda_\rho)}, \\ \sigma_{11}^{21}(\lambda_\rho) &= \frac{(\varepsilon_1\lambda_{1z} - \varepsilon_2\lambda_{2z})(\varepsilon_1\lambda_{1z} + \varepsilon_0\lambda_{0z})e^{d_1\lambda_{1z}}}{2\varepsilon_1\kappa(\lambda_\rho)}, \\ \sigma_{11}^{22}(\lambda_\rho) &= \frac{(\varepsilon_1\lambda_{1z} + \varepsilon_2\lambda_{2z})(\varepsilon_1\lambda_{1z} - \varepsilon_0\lambda_{0z})}{2\varepsilon_1\kappa(\lambda_\rho)}, \\ \sigma_{21}^{21}(\lambda_\rho) &= \frac{\varepsilon_1\lambda_{2z}(\varepsilon_0\lambda_{0z} + \varepsilon_1\lambda_{1z})}{\varepsilon_1\kappa(\lambda_\rho)}, \quad \sigma_{21}^{22}(\lambda_\rho) = \frac{\varepsilon_1\lambda_{2z}(\varepsilon_1\lambda_{1z} - \varepsilon_0\lambda_{0z})e^{d_1\lambda_{1z}}}{\varepsilon_1\kappa(\lambda_\rho)}. \end{aligned}$$

- Source in the bottom layer:

$$\begin{aligned} \sigma_{02}^{12}(\lambda_\rho) &= \frac{2\varepsilon_1\lambda_{1z}\varepsilon_2\lambda_{0z}e^{d_1\lambda_{1z}}}{\varepsilon_2\kappa(\lambda_\rho)}, \\ \sigma_{12}^{22}(\lambda_\rho) &= \frac{\varepsilon_2\lambda_{1z}(\varepsilon_1\lambda_{1z} - \varepsilon_0\lambda_{0z})e^{d_1\lambda_{1z}}}{\varepsilon_2\kappa(\lambda_\rho)}, \quad \sigma_{12}^{12}(\lambda_\rho) = \frac{\varepsilon_2\lambda_{1z}(\varepsilon_0\lambda_{0z} + \varepsilon_1\lambda_{1z})}{\varepsilon_2\kappa(\lambda_\rho)}, \\ \sigma_{22}^{22}(\lambda_\rho) &= \frac{(\varepsilon_0\lambda_{0z} + \varepsilon_1\lambda_{1z})(\varepsilon_2\lambda_{2z} - \varepsilon_1\lambda_{1z}) + (\varepsilon_1\lambda_{1z} - \varepsilon_0\lambda_{0z})(\varepsilon_1\lambda_{1z} + \varepsilon_2\lambda_{2z})e^{2d_1\lambda_{1z}}}{2\varepsilon_2\kappa(\lambda_\rho)}, \end{aligned}$$

where

$$\kappa(\lambda_\rho) = \frac{1}{2}[(\varepsilon_0\lambda_{0z} + \varepsilon_1\lambda_{1z})(\varepsilon_1\lambda_{1z} + \varepsilon_2\lambda_{2z}) + (\varepsilon_0\lambda_{0z} - \varepsilon_1\lambda_{1z})(\varepsilon_1\lambda_{1z} - \varepsilon_2\lambda_{2z})e^{2d_1\lambda_{1z}}].$$

Appendix B. Addition theorems

The following presents the addition theorems, which have been used for the derivation of the ME, LE and corresponding shifting and translation operators of the free space Green’s function (cf. [6,7]). Here, we adopt the definition

$$Y_n^m(\theta, \varphi) = (-1)^m \sqrt{\frac{2n+1}{4\pi} \frac{(n-m)!}{(n+m)!}} P_n^m(\cos \theta) e^{im\varphi} := \widehat{P}_n^m(\cos \theta) e^{im\varphi}, \tag{B.1}$$

for the spherical harmonics where $P_n^m(x)$ (resp. $\widehat{P}_n^m(x)$) is the associated (resp. normalized) Legendre function of degree n and order m . The so-defined spherical harmonics constitute a complete orthogonal basis of $L(\mathbb{S}^2)$ (where \mathbb{S}^2 is the unit spherical surface) and

$$\langle Y_n^m, Y_{n'}^{m'} \rangle = \delta_{nn'} \delta_{mm'}, \quad Y_n^{-m}(\theta, \varphi) = (-1)^m \overline{Y_n^m(\theta, \varphi)}.$$

It is worthy to point out that the spherical harmonics with different scaling constant defined as

$$\widetilde{Y}_n^m(\theta, \varphi) = \sqrt{\frac{(n-|m|)!}{(n+|m|)!}} P_n^{|m|}(\cos \theta) e^{im\varphi} = i^{m+|m|} \sqrt{\frac{4\pi}{2n+1}} Y_n^m(\theta, \varphi), \tag{B.2}$$

have been frequently adopted in published FMM papers (e.g., [11,6,7]).

By the relations

$$k_n(z) = -\frac{\pi}{2} i^n h_n^{(1)}(iz), \quad i_n(z) = i^{-n} j_n(iz), \tag{B.3}$$

and the addition theorems of spherical Bessel functions (cf. [28,29]), we have the following modified addition theorems (cf. [36]).

Theorem B.1. *Let $\mathbf{r}_2 = \mathbf{r}_1 + \mathbf{b}$. Then*

$$k_0(\lambda r_2) = 4\pi \sum_{n=0}^{\infty} \sum_{m=-n}^n (-1)^n k_n(\lambda b) \overline{Y_n^m(\alpha, \beta)} i_n(\lambda r_1) Y_n^m(\theta_1, \varphi_1) \tag{B.4}$$

for $r_1 < b$, and

$$k_0(\lambda r_2) = 4\pi \sum_{n=0}^{\infty} \sum_{m=-n}^n (-1)^n i_n(\lambda b) \overline{Y_n^m(\alpha, \beta)} k_n(\lambda r_1) Y_n^m(\theta_1, \varphi_1) \tag{B.5}$$

for $r_1 > b$.

Theorem B.2. *Let $\mathbf{r}_2 = \mathbf{r}_1 + \mathbf{b}$. Then*

$$i_n(\lambda r_2) Y_n^m(\theta_2, \varphi_2) = \sum_{\nu=0}^{\infty} \sum_{\mu=-\nu}^{\nu} \widehat{S}_{n\nu}^{m\mu}(\mathbf{b}) i_{\nu}(\lambda r_1) Y_{\nu}^{\mu}(\theta_1, \varphi_1), \tag{B.6}$$

where

$$\widehat{S}_{n\nu}^{m\mu}(\mathbf{b}) = 4\pi \sum_{q=0}^{\infty} (-1)^{\nu-n+m+q} i_q(\lambda b) \overline{Y_q^{\mu-m}(\alpha, \beta)} \mathcal{G}(n, m; \nu, -\mu; q), \tag{B.7}$$

with $\mathcal{G}(n, m; \nu, -\mu; q)$ being the Gaunt coefficient.

Theorem B.3. *Let $\mathbf{r}_2 = \mathbf{r}_1 + \mathbf{b}$. Then*

$$k_n(\lambda r_2) Y_n^m(\theta_2, \varphi_2) = \sum_{\nu=0}^{\infty} \sum_{\mu=-\nu}^{\nu} S_{n\nu}^{m\mu}(\mathbf{b}) i_{\nu}(\lambda r_1) Y_{\nu}^{\mu}(\theta_1, \varphi_1), \tag{B.8}$$

for $r_1 < b$, and

$$k_n^{(1)}(\lambda r_2) Y_n^m(\theta_2, \varphi_2) = \sum_{\nu=0}^{\infty} \sum_{\mu=-\nu}^{\nu} (-1)^{\nu-n+m} \widehat{S}_{n\nu}^{m\mu}(\mathbf{b}) k_{\nu}^{(1)}(\lambda r_1) Y_{\nu}^{\mu}(\theta_1, \varphi_1), \tag{B.9}$$

for $r_1 > b$, where $\widehat{S}_{nv}^{m\mu}(\mathbf{b})$ is given by (B.7) and

$$S_{nv}^{m\mu}(\mathbf{b}) = 2\pi^2 (-1)^{m+\nu+1} \sum_{q=0}^{\infty} k_q(\lambda b) \overline{Y_q^{\mu-m}(\alpha, \beta)} \mathcal{G}(n, m; \nu, -\mu; q), \quad (\text{B.10})$$

and $\mathcal{G}(n, m; \nu, -\mu; q)$ is a Gaunt coefficient.

References

- [1] B. Wang, W.Z. Zhang, W. Cai, Fast multipole method for 3-D Helmholtz equation in layered media, *SIAM J. Sci. Comput.* 41 (6) (2020) A3954–A3981.
- [2] B. Wang, W.Z. Zhang, W. Cai, Fast multipole method for 3-D Laplace equation in layered media, *Comput. Phys. Commun.* 259 (2021) 107645.
- [3] H.M. Lin, H.Z. Tang, W. Cai, Accuracy and efficiency in computing electrostatic potential for an ion channel model in layered dielectric/electrolyte media, *J. Comput. Phys.* 259 (2014) 488–512.
- [4] W. Cai, *Computational Methods for Electromagnetic Phenomena: Electrostatics in Solvation, Scattering, and Electron Transport*, Cambridge University Press, New York, NY, 2013.
- [5] A.H. Juffer, E.F.F. Botta, B.A.M.V. Keulen, A.V.D. Ploeg, H.J.C. Berendsen, The electric potential of a macromolecule in a solvent: a fundamental approach, *J. Comput. Phys.* 97 (1) (1991) 144–171.
- [6] L. Greengard, J.F. Huang, A new version of the fast multipole method for screened Coulomb interactions in three dimensions, *J. Comput. Phys.* 180 (2) (2002) 642–658.
- [7] J.F. Huang, J. Jia, B. Zhang, FMM-Yukawa: an adaptive fast multipole method for screened Coulomb interactions, *Comput. Phys. Commun.* 180 (11) (2009) 2331–2338.
- [8] B.Z. Lu, Y.C. Zhou, M.J. Holst, J.A. McCammon, Recent progress in numerical methods for the Poisson-Boltzmann equation in biophysical applications, *Commun. Comput. Phys.* 3 (5) (2008) 973–1009.
- [9] W.M. Brown, P. Wang, S.J. Plimpton, A.N. Tharrington, Implementing molecular dynamics on hybrid high performance computers—short range forces, *Comput. Phys. Commun.* 182 (4) (2011) 898–911.
- [10] L. Greengard, V. Rokhlin, A fast algorithm for particle simulations, *J. Comput. Phys.* 73 (2) (1987) 325–348.
- [11] L. Greengard, V. Rokhlin, A new version of the fast multipole method for the Laplace equation in three dimensions, *Acta Numer.* 6 (1997) 229–269.
- [12] M.H. Cho, W. Cai, A parallel fast algorithm for computing the Helmholtz integral operator in 3-D layered media, *J. Comput. Phys.* 231 (17) (2012) 5910–5925.
- [13] P.J. Li, H. Johnston, R. Krasny, A Cartesian treecode for screened Coulomb interactions, *J. Comput. Phys.* 228 (10) (2009) 3858–3868.
- [14] J. Tausch, The fast multipole method for arbitrary Green's functions, *Contemp. Math.* 329 (2003) 307–314.
- [15] B. Wang, D. Chen, B. Zhang, W.Z. Zhang, M.H. Cho, W. Cai, Taylor expansion based fast multipole method for 3-d Helmholtz equations in layered media, *J. Comput. Phys.* 401 (2020) 109008.
- [16] L.X. Ying, G. Biros, D. Zorin, A kernel-independent adaptive fast multipole algorithm in two and three dimensions, *J. Comput. Phys.* 196 (2) (2004) 591–626.
- [17] L. Wang, R. Krasny, S. Tlupova, A kernel-independent treecode based on barycentric Lagrange interpolation, arXiv:1902.02250.
- [18] O. Bruno, L. Kunyansky, A sparse matrix arithmetic based on \mathcal{H} -matrices. Part I: introduction to \mathcal{H} -matrices, computing, *Computing* 62 (2) (1999) 89–108.
- [19] W. Hackbusch, S. Börm, Data-sparse approximation by adaptive \mathcal{H}^2 -matrices, *Computing* 69 (1) (2002) 1–35.
- [20] S. Chandrasekaran, M. Gu, T. Pals, A fast ULV decomposition solver for hierarchically semiseparable representations, *SIAM J. Matrix Anal. Appl.* 28 (3) (2006) 603–622.
- [21] J.L. Xia, S. Chandrasekaran, M. Gu, X.S. Li, Fast algorithms for hierarchically semiseparable matrices, *Numer. Linear Algebra Appl.* 17 (6) (2010) 953–976.
- [22] D. Chen, W. Cai, An $\mathcal{O}(N \log N)$ hierarchical random compression method for kernel matrices by sampling partial matrix entries, *J. Comput. Phys.* 397 (2019) 108828.
- [23] W.Z. Zhang, B. Wang, W. Cai, Exponential convergence for multipole expansion and translation to local expansions for sources in layered media: 2-D acoustic wave, *SIAM J. Numer. Anal.* 58 (3) (2020) 1440–1468.
- [24] B. Roux, T. Simonson, Implicit solvent models, *Biophys. Chem.* 78 (1–2) (1999 Apr) 1–20.
- [25] M.S. Lee, F.R. Salsbury, M.A. Olson, An efficient hybrid explicit/implicit solvent method for biomolecular simulations, *J. Comput. Chem.* 25 (2004) 1967–1978.
- [26] K. Baker, D. Chen, W. Cai, Investigating the selectivity of KcsA channel by an image charge solvation method (ICSM) in molecular dynamics simulations, *Commun. Comput. Phys.* 19 (4) (2016 Apr) 927–943.
- [27] J. Zavadlav, J. Sablić, R. Podgornik, M. Praprotnik, Open-boundary molecular dynamics of a DNA molecule in a hybrid explicit/implicit salt solution, *Biophys. J.* 114 (10) (2018) 2352–2362.
- [28] G. Watson, *A Treatise of the Theory of Bessel Functions*, second edition, Cambridge University Press, Cambridge, UK, 1966.
- [29] P.A. Martin, *Multiple Scattering: Interaction of Time-Harmonic Waves with N Obstacles*, vol. 107, Cambridge University Press, 2006.
- [30] E.T. Whittaker, G.N. Watson, *A Course of Modern Analysis*, 4th edition, Cambridge University Press, 1927.
- [31] F.W.J. Olver, *NIST Handbook of Mathematical Functions*, Cambridge University Press, 2010.
- [32] M. Abramowitz, I. Stegun, *Handbook of Mathematical Functions*, Dover, New York, 1964.
- [33] J. DeBuhr, B. Zhang, A. Tsueda, V. Tilstra-Smith, T. Sterling, DASHMM: dynamic adaptive system for hierarchical multipole methods, *Commun. Comput. Phys.* 20 (4) (2016) 1106–1126.
- [34] K.A. Michalski, J.R. Mosig, Efficient computation of Sommerfeld integral tails—methods and algorithms, *J. Electromagn. Waves Appl.* 30 (3) (2016) 281–317.
- [35] H. Takahasi, M. Mori, Double exponential formulas for numerical integration, *Publ. RIMS, Kyoto Univ.* 9 (3) (1974) 721–741.
- [36] H.J.H. Clercx, P.P.J.M. Schram, An alternative expression for the addition theorems of spherical wave solutions of the Helmholtz equation, *J. Math. Phys.* 34 (11) (1993) 5292–5302.